

3-Hydroxypyrimidine-2,4-dione-5-N-benzylcarboxamides potently inhibit HIV-1 integrase and RNase H

Bulan Wu, Jing Tang, Daniel J. Wilson, Andrew D. Huber, Mary C Casey, Juan Ji,
Jayakanth Kankanala, Jiashu Xie, Stefan G. Sarafianos, and Zhengqiang Wang

J. Med. Chem., **Just Accepted Manuscript** • DOI: 10.1021/acs.jmedchem.6b00040 • Publication Date (Web): 10 Jun 2016

Downloaded from <http://pubs.acs.org> on June 12, 2016

Just Accepted

“Just Accepted” manuscripts have been peer-reviewed and accepted for publication. They are posted online prior to technical editing, formatting for publication and author proofing. The American Chemical Society provides “Just Accepted” as a free service to the research community to expedite the dissemination of scientific material as soon as possible after acceptance. “Just Accepted” manuscripts appear in full in PDF format accompanied by an HTML abstract. “Just Accepted” manuscripts have been fully peer reviewed, but should not be considered the official version of record. They are accessible to all readers and citable by the Digital Object Identifier (DOI®). “Just Accepted” is an optional service offered to authors. Therefore, the “Just Accepted” Web site may not include all articles that will be published in the journal. After a manuscript is technically edited and formatted, it will be removed from the “Just Accepted” Web site and published as an ASAP article. Note that technical editing may introduce minor changes to the manuscript text and/or graphics which could affect content, and all legal disclaimers and ethical guidelines that apply to the journal pertain. ACS cannot be held responsible for errors or consequences arising from the use of information contained in these “Just Accepted” manuscripts.

1
2
3
4
5
6
7
8
9
10
11
12
13
14
15
16
17
18
19
20
21
22
23
24
25
26
27
28
29
30
31
32
33
34
35
36
37
38
39
40
41
42
43
44
45
46
47
48
49
50
51
52
53
54
55
56
57
58
59
60

3-Hydroxypyrimidine-2,4-dione-5-*N*-benzylcarboxamides potently inhibit HIV-1 integrase and RNase H

Bulan Wu^a, *Jing Tang*^a, *Daniel J. Wilson*^a, *Andrew D. Huber*^b, *Mary C. Casey*^b, *Juan Ji*^b, *Jayakanth Kankanala*^a, *Jiashu Xie*^a, *Stefan G. Sarafianos*^b and *Zhengqiang Wang**

^a

^a Center for Drug Design, Academic Health Center, University of Minnesota, Minneapolis, MN 55455, USA

^b Department of Molecular Microbiology and Immunology and Department of Biochemistry, University of Missouri School of Medicine, Christopher S. Bond Life Sciences Center, Columbia, MO 65211, USA

Abstract

Resistance selection by human immunodeficiency virus (HIV) towards known drug regimens necessitates the discovery of structurally novel antivirals with a distinct resistance profile. Based on our previously reported 3-hydroxypyrimidine-2,4-dione (HPD) core we have designed and synthesized a new integrase strand transfer (INST) inhibitor type featuring a 5-*N*-benzylcarboxamide moiety. Significantly, the 6-alkylamino variant of this new chemotype consistently conferred low nanomolar inhibitory activity against HIV-1. Extended antiviral testing against a few raltegravir-resistant HIV-1 clones revealed a resistance profile similar to that of the second generation INST inhibitor (INSTIs) dolutegravir. Although biochemical testing and molecular modeling also strongly corroborate the inhibition of INST as the antiviral mechanism of action, selected antiviral analogues also potently inhibited reverse transcriptase (RT) associated RNase H, implying potential dual target inhibition. *In vitro* ADME assays demonstrated that this novel chemotype possesses largely favorable physicochemical properties suitable for further development.

Introduction

HIV infects an estimated 34 million people worldwide. Clinical management of HIV / AIDS continues to rely on highly active antiretroviral therapy (HAART) that consists of five different classes of FDA-approved drugs¹: nucleoside reverse transcriptase inhibitors (NRTIs); nonnucleoside reverse transcriptase inhibitors (NNRTIs); protease inhibitors (PIs); INSTIs; and entry inhibitors. However, HIV infection remains incurable²⁻³ due to the persistence of viral reservoirs. The resulting long duration of HAART typically amounts

1
2
3 to two treatment challenges: toxicities and the selection of resistant viral strains. The
4 emergence of multidrug resistance is particularly concerning as treatment options will be
5 severely limited. Therefore, sustained success in HIV HAART requires novel antivirals
6 with structurally unique pharmacophore and distinct resistance profile. HIV IN plays
7 critical roles in viral infection and the establishment of proviral latency.⁴⁻⁶ As an antiviral
8 target IN is particularly attractive because 1) there is no host cellular counterpart, hence
9 specific inhibitors should not interfere with cellular functions; and 2) IN uses the same
10 active site (DD35E motif) for both the 3' processing and the ST steps, therefore, inhibitors
11 could benefit from a potentially high genetic barrier to resistance selection. Specific INSTIs
12 all feature a diketoacid (DKA) functionality or its heterocyclic bioisosteres⁷⁻¹¹ along with
13 a hydrophobic terminal benzyl moiety,¹²⁻¹⁷ as demonstrated by all three FDA-approved
14 INSTIs (Figure 1): raltegravir (**1**)¹⁸⁻¹⁹, elvitegravir (**2**),²⁰ and dolutegravir (**3**).²¹⁻²²
15 Particularly significant is the second-generation INSTI **3** which retains potency against
16 many raltegravir-resistant HIV strains.²³ We have previously developed a few chemotypes
17 featuring the HPD core²⁴⁻²⁷ that effectively inhibited HIV-1 in cell culture. The antiviral
18 potency associated with these HPD subtypes is likely due to the dual inhibition of RT and
19 IN as indicated by biochemical assays. However, the IN inhibition was typically much
20 weaker than the inhibition of RT. Furthermore, cross resistance to **1** was also observed,
21 suggesting that these early HPD subtypes may have the characteristics of first-generation
22 INSTIs. Another variant of HPD was recently found to selectively inhibit the RT-
23 associated RNase H without significantly inhibiting INST.²⁸ We report herein a rationally
24 designed new HPD variant (Figure 1, **4**) featuring a unique C5 carboxamide moiety to
25 specifically inhibit INST. Significantly, chemotype **4** has the two structural determinants
26
27
28
29
30
31
32
33
34
35
36
37
38
39
40
41
42
43
44
45
46
47
48
49
50
51
52
53
54
55
56
57
58
59
60

essential for INST binding and inhibition (Figure 1). The overall shape and functionalities of **4** particularly resemble those of **3**, suggesting that our novel inhibitors can be second generation INSTIs.

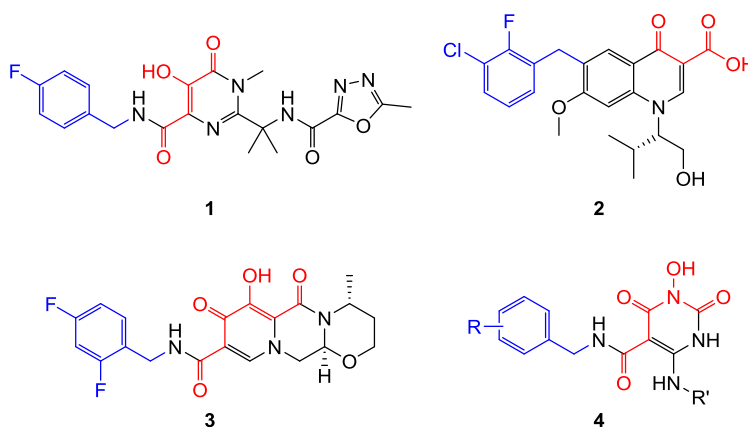


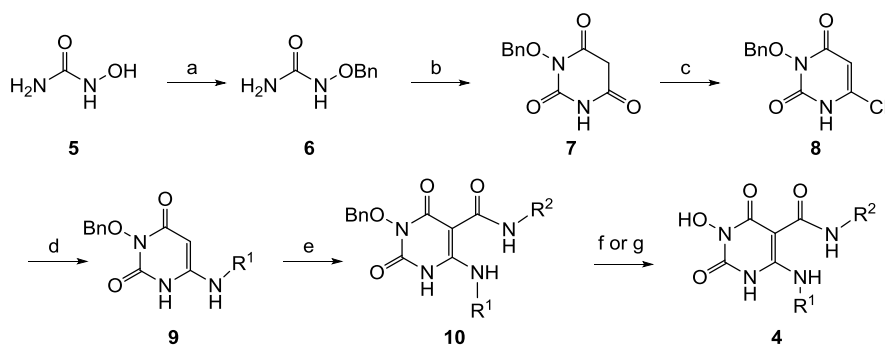
Figure 1. Structures of FDA-approved INSTIs: raltegravir (**1**), elvitegravir (**2**), dolutegravir (**3**), and our newly designed HPD inhibitor subtype **4**. Each approved drug features a chelating traid (red) and a terminal benzyl group (blue) that constitute the pharmacophore of HIV-1 INSTIs. Chemotype **4** fits the pharmacophore with the same two structural features.

Results and Discussion

Chemistry. Our target compounds **4** were prepared via a concise and diverse synthetic route shown in Scheme 1. The synthesis started from commercially available hydroxyurea **5** which was *O*-benzylated with BnBr in the presence of KOH under reflux to provide 1-(benzyloxy)urea **6** in high yield.²⁹ Cyclocondensation of 1-(benzyloxy)urea **2** and diethyl malonate provided six-membered heterocycle compound 3-(benzyloxy)-6-hydroxypyrimidine-2,4(1H,3H)-dione **7** in moderate yield under microwave irradiation (150 °C, 20 min) or under conventional heating (reflux, overnight).³⁰ Compound **7** was converted to key intermediate 3-(benzyloxy)-6-chloropyrimidine-2,4(1H,3H)-dione **8** by

reacting with POCl₃ in the presence of BnEt₃NCl.³¹ Reaction of intermediate chloride **8** with amines in the presence of N,N-dimethylaniline under microwave condition provided 6-amination products **9** in moderate to good yield.³² The key C5 carboxamide was introduced by reacting 6-amino intermediates **9** with commercial or *in situ* generated isocyanates (Scheme 1),³³ a highly efficient method for small scale synthesis of intermediate **10**. The final debenzoylation was achieved by treating compounds **10** with TFA under microwave condition³⁴ or via catalytic hydrogenation.

Scheme 1^a Synthesis of chemotype **4**

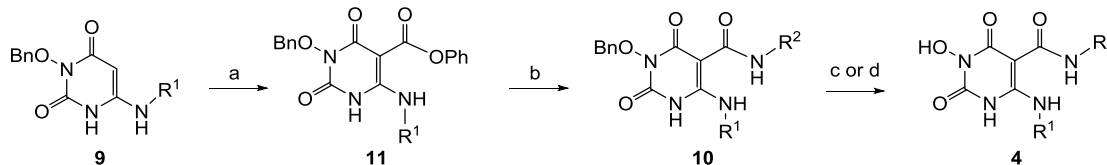


^a Reagents and conditions: a) KOH, BnBr, MeOH, reflux, 6 h, 91%; b) CH₂(COOEt)₂, NaOEt, MW, 150 °C, 20 min, 58%; c) POCl₃, BnEt₃NCl, 50 °C, 6 h, 88%; d) R¹-NH₂, N,N-dimethylaniline, MW, 170 °C, 20–25 min, 54–78%; e) R²NCO (or R²CON₃), PhNO₂, MW, 210 °C, 20–40 min, 60–100%; f) Pd/C, H₂, 40–50 Psi, MeOH, 4–6 h, 82–97%; g) TFA, MW, 120 °C, 35–55 min, 50–77%.

Alternatively, the C5 carboxamidation can be achieved via a two-step reaction sequence (scheme 2) to avoid the use of the unpleasant nitrobenzene. In this case, the amino intermediate **9** was first treated with phenyl chloroformate and a base, such as pyridine, to give intermediate phenyl ester **11** which was converted to amide **10** upon reacting with a

primary amine under conventional heating or microwave conditions. Debenzylation with the same protocol afforded the desired chemotype **4**.

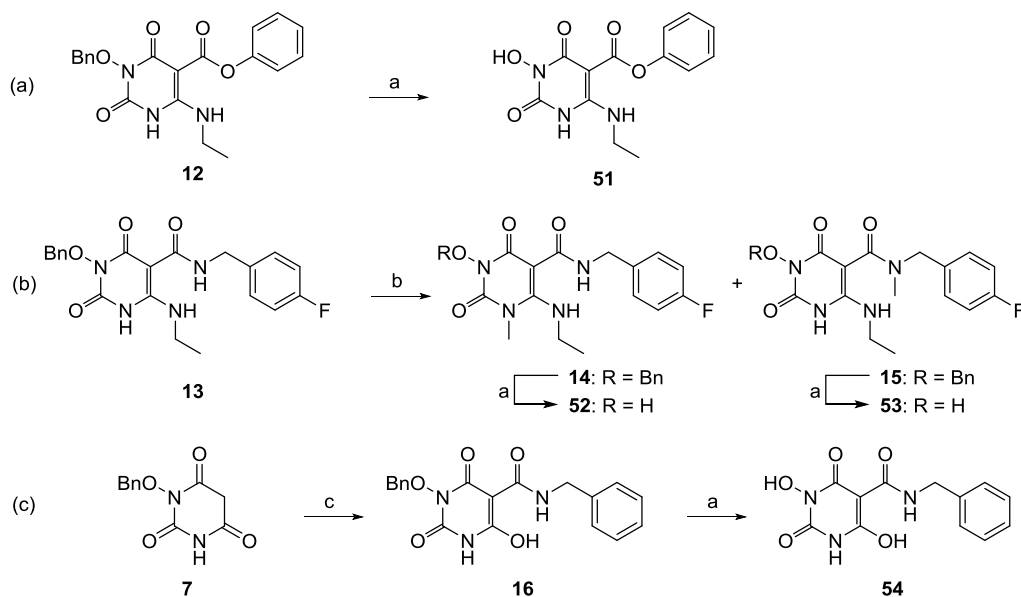
Scheme 2^a Alternative synthesis of chemotype **4**



^aReagents and conditions: a) ClCO₂Ph, pyridine, rt, 2h, 62%; b) R²-NH₂, MW, dioxane, 100 °C, 50 min, 82–92%; c) Pd/C, H₂, 40~50 Psi, MeOH, 4–6 h, 82–97%; d) TFA, MW, 120 °C, 35–55 min, 50–77%.

Meanwhile our analogue synthesis also included a few variants of **4** which entailed slightly different synthetic routes or further functionalization (Scheme 3). In these events, direct debenzylation of intermediate **12** afforded compound **51** (Scheme 3, a), whereas methylation of intermediate **13** produced two regio-isomers **14** and **15**, which upon debenzylation yielded compounds **52** and **53**, respectively (Scheme 3, b). Interestingly, a 6-deamino analogue **54** was also synthesized from intermediate **7** via the carboxamidation and debenzylation sequence (Scheme 3, c).

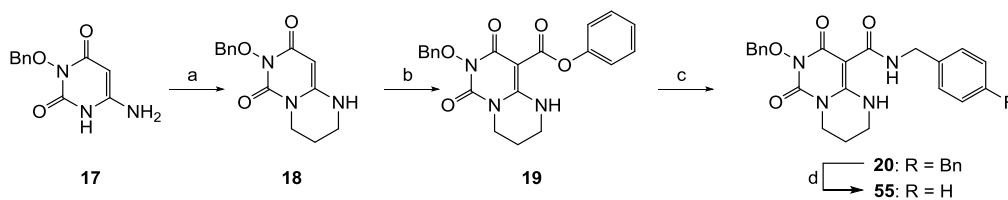
Scheme 3^a Synthesis of compounds **51–54**



^aReagents and conditions: a) TFA, MW, 120 °C, 35–55 min; b) MeI, Cs₂CO₃, DMSO, rt, 2h; c) benzyl isocyanate, ^tPr₂NEt, DCM, rt, 3h.

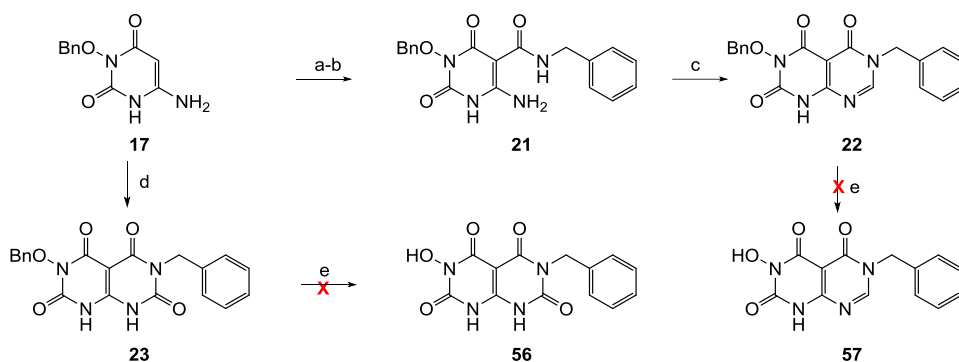
Finally, synthesis of analogues (**55–57**) with another six-membered ring fused to the HPD core via N1-C6 (**55**) or C6-C5 (**56–57**) was also attempted. Compound **55** was synthesized from 6-amino HPD intermediate **17** which was cyclized to **18** upon treating with 1,3-dibromopropane under basic condition (Scheme 4). The rest of the synthesis involved the same carboxamidation–debenzylation sequence as used for the synthesis of chemotype **4**. The synthesis of C6-C5 fused analogues (**56–57**) was attempted based on Scheme 5. While the two intermediates **22–23** were obtained, the subsequent debenzylation was unsuccessful (Scheme 5).

Scheme 4^a Synthesis of compound **55**



^aReagents and conditions: a) 1,3-dibromopropane, K₂CO₃, DMF, 60 °C, 2h, 90%; b) phenyl chloroformate, pyridine, rt, 3 h, 86%; c) 4-fluorobenzylamine, MW, dioxane, 100 °C, 50 min, 91%; d) TFA, MW, 120 °C, 35 min, 96%.

Scheme 5^a Attempted synthesis of compounds **56–57**

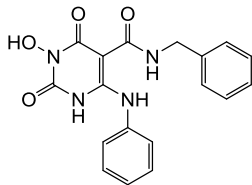


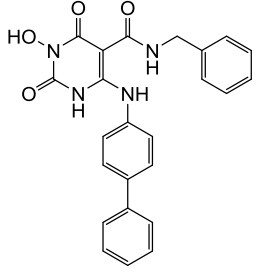
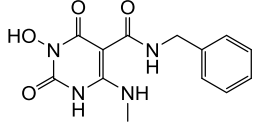
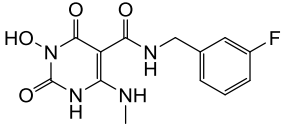
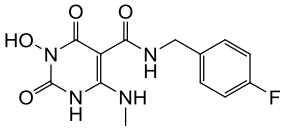
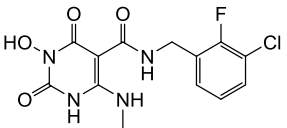
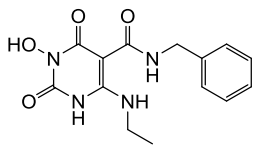
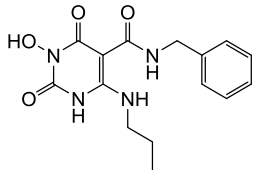
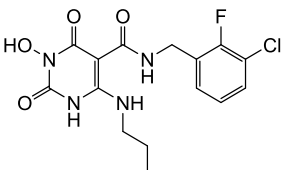
^aReagents and conditions: a) ClCO₂Ph, pyridine, rt, 2h; b) BnNH₂, MW, dioxane, 100 °C, 50 min, 76%; c) HC(OEt)₃, CF₃CO₂H (cat.), MW 150 °C, 10 min, 49%; d) BnNCO, PhNO₂, MW 210 °C, 10 min, 62%; e) TFA, MW, 120 °C, 35–55 min; or Pd/C, H₂, 40–50 Psi, MeOH, 4–6 h.

Biology. All final compounds (**24–55**) were first screened in a viral cytopathic effect (CPE) based antiviral assay against HIV-1_{IIIB} in CEM-SS cells.³⁵⁻³⁶ In this assay, the reduction of CPE was used to indicate the antiviral activity of a compound. The screening was conducted under single concentration (10 μM) and the percent inhibition and percent cell viability were calculated using a virus control and cell control, respectively. Best compounds from this assay were further evaluated in a single replication cycle MAGI assay. In addition, all compounds were tested in a biochemical assay with recombinant HIV-1 IN measuring INST activity. Selected ones were also tested against RT-associated RNase H activity. Both **3** and **1** were included in all assays as reference compounds. The results indicate a few prominent structure-activity-relationship (SAR) trends.

Alkylamino group is required at C6. From the antiviral screening assay, the most striking SAR was that the two analogues with an aromatic amine at the C6 position (**24–25**) were completely inactive and largely cytotoxic in the cytoprotection antiviral assay, whereas a small aliphatic amine substitution at the same position (**26–37**, Table 1) conferred excellent antiviral activity without cytotoxicity, with the lone exception being the *t*-butylamino analogue (**42**) which was inactive and cytotoxic. The same dramatic SAR was observed from the INST biochemical assay in which neither of the arylamino analogues (**24–25**) showed appreciable inhibition at concentrations up to 100 μM whereas the alkylamino analogues (**26–37**) all demonstrated nanomolar inhibitory activity, including the *t*-butylamino analogue (**35**). Furthermore, although most alkyl analogues (**26–31**, **33–34**) produced maximal cytoprotection at 10 μM without significant cytotoxicity, linear alkyl substituted analogues (**26–31**) are generally favored in the INST biochemical assay over the unsubstituted analogue (**36**) and the bulky alkyl substituted ones, such as the isopropyl (**33**) and cyclopropyl (**34**) groups. Biochemical analysis also showed that the ethyl substituent (**30**) confers the best inhibition against INST ($\text{IC}_{50} = 33 \text{ nM}$).

Table 1. SAR of the C6 amino group: antiviral screening and biochemical assay of **24–36**

Compd	Structure	Antiviral Screening (10 μM) ^a		INST IC_{50} (μM) ^b
		CPE reduction %	viability %	
24		0	21	>100

1					
2					
3					
4					
5					
6					
7					
8	25		0	13	>100
9					
10					
11					
12					
13					
14					
15	26		100	98	0.080 ± 0.007
16					
17					
18					
19					
20	27		100	95	0.25 ± 0.048
21					
22					
23					
24					
25					
26	28		100	89	0.11 ± 0.021
27					
28					
29					
30	29		100	100	0.11 ± 0.033
31					
32					
33					
34					
35					
36					
37	30		100	100	0.033 ± 0.004
38					
39					
40					
41					
42					
43	31		100	97	0.066 ± 0.016
44					
45					
46					
47					
48					
49					
50	32		33	48	0.058 ± 0.012
51					
52					
53					
54					
55					
56					
57					
58					
59					
60					

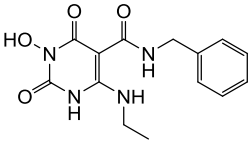
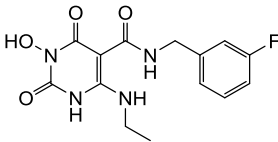
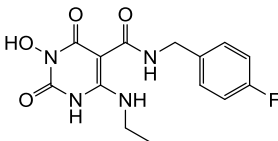
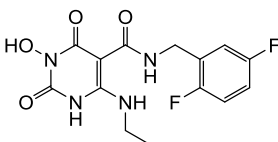
33		98	90	0.15 ± 0.034
34		98	91	0.21 ± 0.077
35		0	17	0.081 ± 0.015
36		99	100	0.90 ± 0.29
3	--	--	--	0.068 ± 0.01
1	--	--	--	0.65 ± 0.14

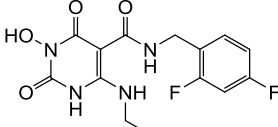
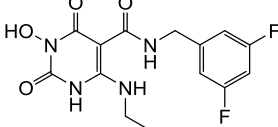
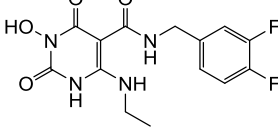
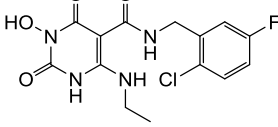
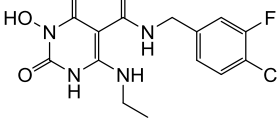
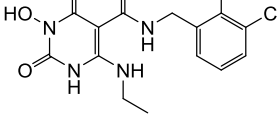
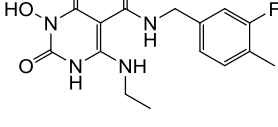
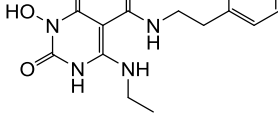
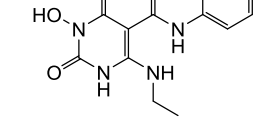
^a Cytoprotection assay using HIV-1 IIB in CEM-SS cells with a viral control for CPE reduction and cell control for cell viability. ^b Concentration inhibiting INST by 50%, expressed as mean ± standard deviation from at least three independent experiments.

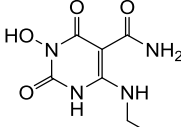
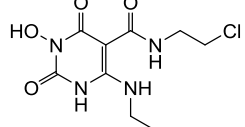
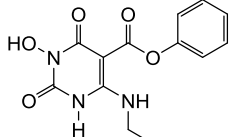
N-Benzyl substitution on the C5 carboxamide is highly desired. To explore the SAR concerning the C5 carboxamide moiety, analogues of compound **30** were synthesized and tested in the antiviral screening assay and the INST biochemical assay (Table 2). Remarkably, all analogues with a benzyl group on the C5 carboxamide (**30**, **37–46**) demonstrated maximal cytoprotection (92–100%) without considerable cytotoxicity (cell viability 87–100%), with the only exception being compound **43** which provided 62% cytoprotection with 73% cell viability at 10 μM. Consistent with the maximal

cytoprotection, exceptional biochemical inhibition ($IC_{50} = 21\text{--}230\text{ nM}$) was also observed for these analogues. Interestingly, compound with an extra methylene group (**47**) also produced maximal cytoprotection at $10\text{ }\mu\text{M}$, though the biochemical inhibition was substantially reduced (**47** vs **30**). In stark contrast, replacing the benzyl group with a phenyl ring (**48**), alkyl group (**50**), or removing the *N*-substituent (**49**) completely abrogated both the antiviral activity and biochemical inhibition. Compound with a C5 phenyl ester (**51**) was also devoid of biochemical inhibition and yielded 50% cytoprotection at $10\text{ }\mu\text{M}$. All these SAR observations are well aligned with the known pharmacophore model of INSTIs.

Table 2. SAR around the C5 carboxamide: antiviral screening and biochemical assay of **30** analogues **47–51**

Compd	Structure	Antiviral Screening ($10\text{ }\mu\text{M}$) ^a		INST IC_{50} (μM) ^b
		CPE reduction %	viability %	
30		100	100	0.033 ± 0.004
37		100	90	0.068 ± 0.007
38		100	99	0.049 ± 0.004
39		92	87	0.068 ± 0.011

1					
2					
3					
4					
5	40		100	92	0.048 ± 0.007
6					
7					
8					
9					
10	41		100	100	0.23 ± 0.062
11					
12					
13					
14					
15					
16	42		100	100	0.077 ± 0.011
17					
18					
19					
20					
21					
22	43		62	73	0.095 ± 0.019
23					
24					
25					
26					
27					
28	44		100	100	0.12 ± 0.021
29					
30					
31					
32					
33					
34	45		100	100	0.021 ± 0.002
35					
36					
37					
38					
39					
40	46		100	100	0.051 ± 0.013
41					
42					
43					
44					
45	47		99	87	0.10 ± 0.03
46					
47					
48					
49					
50					
51	48		11	27	35 ± 17
52					
53					
54					
55					
56					
57					
58					
59					
60					

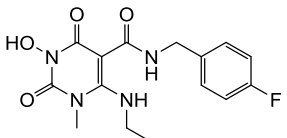
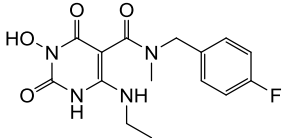
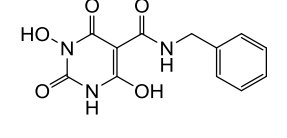
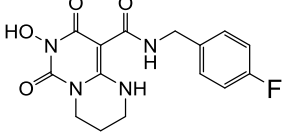
49		--	--	>100
50		5.1	100	>100
51		50	100	>100
3	--	--	--	0.068 ± 0.01
1	--	--	--	0.65 ± 0.14

^a Cytoprotection assay using HIV-1 IIIB in CEM-SS cells with a viral control for CPE reduction and cell control for cell viability. ^b Concentration inhibiting INST by 50%, expressed as mean ± standard deviation from at least three independent experiments.

Scaffold analogues lack antiviral activity or biochemical INST inhibition. To further confirm the SAR trends shown in Tables 1–2, we also synthesized a few scaffold analogues of the new chemotype. Compounds **52–53** were synthesized to explore the impact of methylation on N1 or the C5 carboxamide. Remarkably, a simple methylation at N1 completely abrogated the antiviral activity, cell viability and the biochemical inhibition (**52**). Methylation of the C5 carboxamide also caused a complete loss of antiviral activity while substantially attenuating the biochemical inhibition (**53** vs **38**). Similarly, the 6-deamino analogue **61** demonstrated drastically reduced antiviral potency and biochemical inhibition (**54** vs **30**), confirming the importance of the amino group at C6 for biological

activities. Finally, cyclized analogue **55** was inactive and cytotoxic in the antiviral screening assay, though the biochemical inhibition was largely preserved ($IC_{50} = 430$ nM).

Table 3. Antiviral screening and biochemical assay of scaffold analogues **52–55**

Compd	Structure	Antiviral Screening ($10 \mu M$) ^a		INST IC_{50} (μM) ^b
		CPE reduction %	viability %	
52		6.5	10	>100
53		0	89	7.0 ± 3.3
54		26	100	37 ± 21
55		0	5.5	0.43 ± 0.13

^a Cytoprotection assay using HIV-1 IIIB in CEM-SS cells with a viral control for CPE reduction and cell control for cell viability. ^b Concentration inhibiting INST by 50%, expressed as mean \pm standard deviation from at least three independent experiments.

Dose response antiviral testing. To better gauge the antiviral potency, selected inhibitors with excellent CPE reduction and cell viability from the antiviral screening assay were further tested in a dose response fashion, from which the EC_{50} and CC_{50} were determined (Table 4). All compounds tested showed nanomolar activity and five of the eight analogues

1
2
3 were active in low nanomolar range ($EC_{50} = 15\text{--}61$ nM). Although these analogues showed
4 mild cytotoxicity with CC_{50} s in the range of $18\text{--}58$ μM , the selectivity window (Table 4),
5 particularly that for analogues **40** (TI = 1500) and **45** (TI = 1200), is sufficiently large to
6 warrant their further development. To confirm the observed antiviral potency, these same
7 analogues were further evaluated in a distinct MAGI assay.³⁶⁻³⁷ This assay measures HIV
8 infection in indicator cells (P4R5) through the expression of a Tat-dependent reporter (β -
9 galactosidase) and requires only one replication cycle. While the EC_{50} values were
10 generally higher in this assay, our compounds still demonstrated nanomolar antiviral
11 potency with the exception of compounds **26** and **46**. Interestingly, compound **45**, while
12 showing the best potency in both the INST assay and the CPE antiviral assay, exhibited a
13 significantly higher EC_{50} (0.30 μM vs 0.015 μM) in the MAGI assay. By comparison, EC_{50}
14 values for analogues **38** and **40** were comparable to **1** in the CPE assay and only 2-5 fold
15 higher than **3** and **1** in the MAGI assay. Nevertheless, dose response antiviral testing in two
16 distinct assays confirmed a highly potent antiviral profile of our newly designed
17 compounds.
18
19
20
21
22
23
24
25
26
27
28
29
30
31
32
33
34
35
36
37
38
39
40
41

Table 4. Dose-response antiviral results of selected analogues from two different assays

Compound	Cytoprotection Assay ^a			MAGI Assay ^b
	EC_{50} (μM) ^c	CC_{50} (μM) ^d	TI ^e	EC_{50} (μM) ^f
26	0.83	58	70	3.7 ± 0.3
30	0.061	23	380	0.30 ± 0.01
38	0.033	19	580	0.090 ± 0.02

40	0.032	47	1500	0.070 ± 0.02
42	0.049	21	430	0.30 ± 0.06
44	0.19	19	100	0.80 ± 0.2
45	0.015	18	1200	0.30 ± 0.09
46	0.15	20	130	1.3 ± 0.2
3	--	--	--	0.020 ± 0.002
1	0.023	>10	>430	0.030 ± 0.008

^a Concentration inhibiting INST by 50%, ^c Concentration of a compound inhibiting virus replication by 50%. ^d Concentration of a compound resulting in 50% cell death. ^e Therapeutic index, defined as CC₅₀/EC₅₀. ^f Expressed as mean ± standard deviation from two independent experiments.

Antiviral resistance profile. Mutations conferring resistance to INSTIs have been generated in cell culture and emerged in clinical studies.³⁸⁻⁴⁰ To establish the resistance profile of chemotype **4**, a representative compound **45** was evaluated for antiviral potency against four raltegravir-resistant HIV-1 clones⁴¹ in the CPE assay. These clones contain one or more major mutations in HIV-1 IN that are associated with raltegravir resistance,^{23, 24} namely a Y143C or an N155H single mutation; a G140S / Q148H double mutation and a G140S / Y143H / Q148H triple mutation. AZT, **1** and **3** were included in the study for comparison purpose. The results are summarized in Table 5. As expected cross-resistance to **1** was not observed for AZT due to its orthogonal mechanism of action as an NRTI, whereas the resistance profile observed in our antiviral assay for **3** is largely consistent

with the reported profile.²³ Similar to **3**, compound **45** retains its potency against clones with only one major IN mutation (clones 1556-1 and 4736-2) while HIV-1 clones with IN double mutations (clone 8070-1) and triple mutations (clone 8070-1) demonstrated moderate resistance to **45**, with fold resistance of 13 and 6.3, respectively. The fold-resistance of **45** is strikingly similar to that observed with **3** for each of the four HIV-1 clones (Table 5). These observations strongly suggest that our chemotype **4** may confer antiviral activity via inhibiting INST in a manner similar to that of **3**, a second generation INSTI.⁴²

Table 5. Resistance profile of **45** against raltegravir-resistant HIV-1 clones

HIV-1 Clone	Major Mutations	Fold-resistance ^a			
		45	AZT	1	3
1556-1	Y143C	0.4	1.4	170	2.0
4736-2	N155H	2.4	0.7	14	1.8
8070-1	G140S / Y143H / Q148H	6.3	0.9	220	9.6
8070-2	G140S / Q148H	13	0.5	145	12

^a Fold-resistance is defined as $EC_{50}(\text{mutant}) / EC_{50}(\text{WT})$.

Inhibition against RT-associated RNase H. Consistent with the aforementioned antiviral profile against raltegravir-resistant HIV-1 clones, which implies an antiviral mechanism of action (MOA) similar to second generation INSTI **3**, biochemical data also closely correlate with the observed antiviral activity, as each of the selected analogues exhibited a

1
2
3 biochemical IC₅₀ against INST very similar to the antiviral EC₅₀, particularly from the CPE
4 assay (Table 6). In addition, none of the inactive compounds (**24–25**, **48** and **50–54**) from
5 the CPE antiviral assay inhibited INST (Tables 1–3), strongly suggesting that our new
6 compounds target INST. However, HIV IN and RNase H share a similar active site fold,⁴³
7 hence their inhibition entails similar pharmacophore elements, mainly a chelating triad and
8 a hydrophobic aromatic moiety. Therefore, we also tested selected analogues in another
9 biochemical assay measuring the RNase H function of RT. Remarkably, all these analogues
10 demonstrated exceptional biochemical inhibition against RNase H with IC₅₀s in the low
11 nanomolar range (10–61 nM, Table 6), which correlates with the antiviral activity as well
12 as the INST inhibition does in general. By contrast, the two reference compounds, **3** and **1**,
13 did not inhibit RNase H significantly at concentrations up to 10 μM. These observations
14 indicate that the exceptional antiviral potency of our new chemotype could be due to dual
15 target inhibition. Further virological characterizations of our compounds, including MOA
16 studies via viral passage experiments for resistance selection, are currently underway and
17 will be reported in due course.

18
19
20
21
22
23
24
25
26
27
28
29
30
31
32
33
34
35
36
37
38
39 **Table 6.** Biochemical inhibition of RT-associated RNase H and the antiviral correlation

<i>Compound</i>	<i>RNase H</i> <i>IC₅₀ (μM)^a</i>	<i>INST</i> <i>IC₅₀ (μM)^a</i>	<i>CPE</i> <i>EC₅₀ (μM)^b</i>	<i>MAGI</i> <i>EC₅₀ (μM)^c</i>
26	0.061 ± 0.004	0.080 ± 0.007	0.83	3.7 ± 0.3
30	0.042 ± 0.012	0.033 ± 0.004	0.061	0.30 ± 0.01
38	0.011 ± 0.003	0.049 ± 0.004	0.033	0.09 ± 0.02

40	0.010 ± 0.006	0.068 ± 0.011	0.032	0.07 ± 0.02
42	0.026 ± 0.009	0.077 ± 0.011	0.049	0.30 ± 0.06
44	0.022 ± 0.009	0.12 ± 0.021	0.19	0.80 ± 0.2
45	0.029 ± 0.015	0.021 ± 0.002	0.015	0.30 ± 0.09
46	0.020 ± 0.010	0.051 ± 0.013	0.15	1.3 ± 0.2
3	>10	0.068 ± 0.01	--	0.020 ± 0.002
1	>10	0.65 ± 0.14	0.023	0.030 ± 0.008

^a Concentration with 50% enzyme inhibition, expressed as mean ± standard deviation from three independent experiments. ^b Concentration of a compound inhibiting virus replication by 50%. ^c Concentration of a compound inhibiting virus replication by 50%, expressed as mean ± standard deviation from three independent experiments.

Mechanism of strand transfer inhibition. HIV IN is a 32-kDa protein encoded by viral pol gene consisting of three functional domains⁴⁴: the N-terminal domain (NTD) with a conserved “HH-CC” zinc-binding motif; the catalytic core domain (CCD) containing the key D64-D116-E152 catalytic triad; and the C-terminal domain (CTD) important for DNA binding. Although crystal structures of each single domain as well as double domains had been reported,⁴⁵⁻⁴⁷ detailed understanding on HIV INST catalysis and inhibition remained elusive until the disclosure of crystal structures of full-length IN and viral DNA complex (intasome) for a homologous prototype foamy virus (PFV).⁴⁸⁻⁴⁹ Homologous models⁵⁰⁻⁵¹ constructed based on these PFV intasome crystal structures have provided valuable details into HIV INST mechanism of action and formed the basis for structure-based INSTI

design. Significantly these models corroborate the minimal pharmacophore embedded in major INSTIs as shown in Figure 1.

To illustrate the binding mode of our new chemotype at HIV IN active site, we have performed molecular docking on a representative analogue **45** using a PFV intasome model (Figure 2).⁵⁰ Significantly, **45** fits perfectly into the IN binding site through two major binding domains: the 3-N hydroxyl group simultaneously chelates to both Mg²⁺ ions while allowing the placement of the benzyl group into the protein-DNA interfacial hydrophobic pocket involving π -stacking of the i) fluorobenzyl side chain with the deoxycytosine C16 of viral DNA, and ii) π -stacking of the central uracil ring with the terminal 3'-deoxyadenosine A17 (Figure 2a). In addition, a structure overlay of **45** with **3** reveals a high degree of similarity between their binding (Figure 2b), suggesting that our new molecular scaffold can effectively engage with HIV IN for ST inhibition.

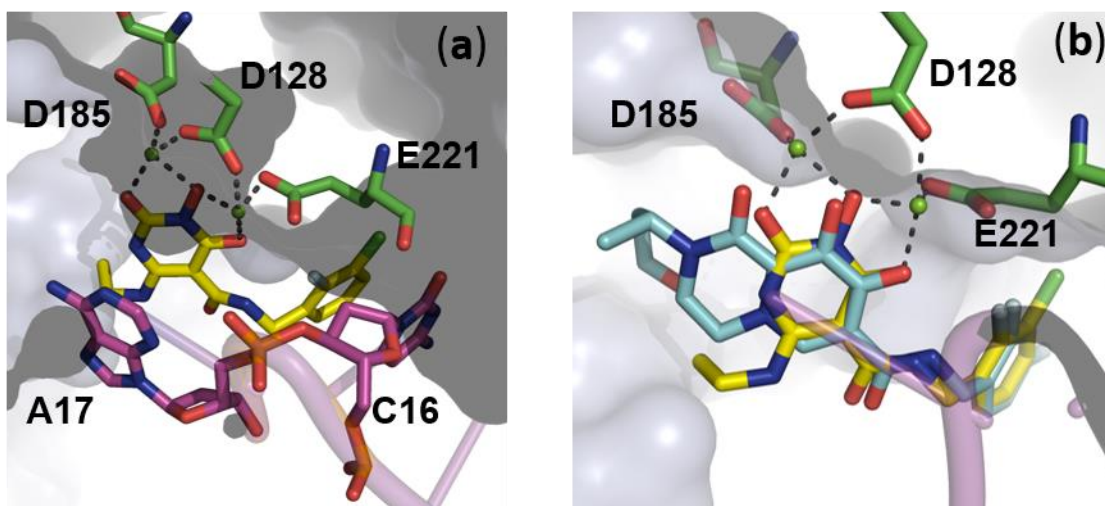


Figure 2. a) Predicted binding mode of **45** (yellow) as obtained by molecular docking in the PFV intasome catalytic site (PDB code: 3S3M).⁵⁰ Magnesium cations depicted in green spheres, catalytic residues in green sticks and viral DNA in magenta cartoon. b) Overlay

of **45** (yellow) and crystallographic **3** (cyan) in the catalytic active site of PFV intasome (PDB code: 3S3M) with Mg^{2+} ions in green spheres and viral DNA in magenta cartoon. Numbering in black is in accordance to the PFV intasome crystal structure (PDB code: 3S3M).

To understand the effect of mutations on antiviral profile of **1** and **45**, molecular modeling was performed with these two compounds into the PFV IN Y212C mutant which corresponds to the Y143C of HIV IN (Figure 3). It was observed that the oxadiazole moiety of **1** makes a critical π - π stack interaction with Y143 (Figure 3a). This interaction is not available with the C143 residue and the binding of **1** to the Y143C mutant is significantly weakened (Figure 3b). On the other hand, **45** lacks the oxadiazole moiety to interact with Y143 (Figure 3a). Consequently, the Y143C mutation would not impact its binding to IN. These docking studies are consistent with the observations that Y143 mutation confers major resistance to **1** and no resistance to **45** (Table 5).

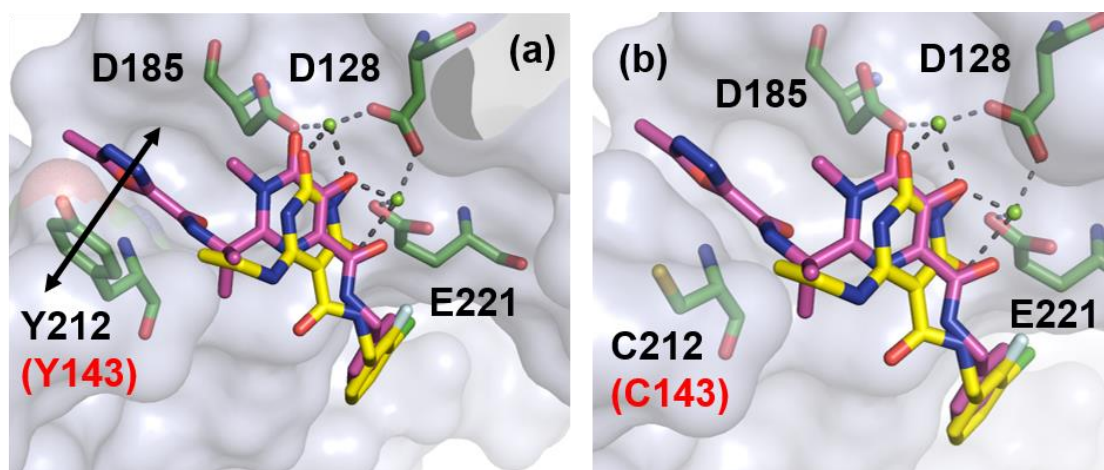


Figure 3. a) Overlay of **1** (magenta) and **45** (yellow) within the PFV IN active site in complex with magnesium (green spheres) (PDB code: 3OYA). π - π stack interaction between oxadiazole moiety within **1** and Y212 is shown by black double headed arrow. b)

1
2
3 Overlay of **1** (magenta) and **45** (yellow) within the active site of PFV IN Y212C
4
5 (corresponding to HIV IN Y143C) mutant. Key residues (D128, D185, E221 and Y212) are
6
7 represented as green sticks. Numbering in black is in accordance to the PFV intasome
8
9 crystal structure (PDB code: 3S3M). The corresponding numbering for HIV IN is
10
11 highlighted in red.
12
13

14
15 **Physicochemical and *in vitro* ADME.** To assess drug-like properties of chemotype **4**,
16
17 selected analogues were tested in various physicochemical and *in vitro* ADME studies
18
19 (Table 7). First, aqueous stability and solubility were evaluated in Dulbecco's Phosphate-
20
21 Buffered Saline (DPBS). The selected compounds showed excellent stability and good
22
23 solubility in DPBS with the exception of **45** showed a lower but still acceptable solubility.
24
25 Second, the selected compounds were found to be stable in both human and mouse plasma.
26
27 Third, all compounds showed a higher protein binding in human plasma (98-99%) than
28
29 that in mouse plasma (71-96%). Finally, while the selected compounds exhibited excellent
30
31 phase I stability in both human and mouse liver microsomes, they were much less stable
32
33 against phase II glucuronidation in microsomes from both species (Table 7). Taken
34
35 together, although the selected compounds still need improvement in their phase II
36
37 glucuronidation stability, they possess largely favorable physicochemical and *in vitro*
38
39 ADME properties. It is also noteworthy that our chemotype has a significant smaller size
40
41 (MW for **45** = 322; the MW for drugs **1–3** is in the range of 419–448) while supporting
42
43 antiviral activities comparable to **1** (Table 4). The small size of our chemotype would allow
44
45 significant room for further optimization.
46
47
48
49
50
51
52

53 **Table 7.** Physicochemical and *in vitro* ADME profile of selected analogues
54
55
56
57
58
59
60

Compd	Aqueous Solubility (μM)	Aqueous Stability t _{1/2} (h)	Plasma Stability t _{1/2} (h)		Plasma Protein Binding (%) ^a		Microsomal Stability (Phase I / Phase II, CL _{int}) ^b	
			Human	Mouse	Human	Mouse	Human	Mouse
26	138	> 24	> 24	> 24	99.2	70.9	0.8 / 51	< 0.1 / 500
30	1091	> 24	> 24	> 24	99.1	83.9	< 0.1 / 355	< 0.1 / 732
38	150	> 24	> 24	> 24	99.4	86.5	< 0.1 / 336	< 0.1 / 1240
45	11	> 24	> 24	> 24	98.4	94.0	< 0.1 / 850	< 0.1 / 1065
46	81	> 24	> 24	> 24	98.9	95.9	< 0.1 / 357	0.4 / 1342

^a Percent of fraction bound.

^b CL_{int}: intrinsic clearance, μl/min/mg protein.

Conclusion. A new HPD subtype was designed and synthesized. Key to the design is the introduction of an *N*-benzyl-5-carboxamide moiety to mimic the second-generation INSTI **3**. SAR revealed the requirement of an alkylamino group at C6 and an *N*-benzyl group on the C5 carboxamide for INST inhibition and antiviral activity. Numerous analogues demonstrated low nanomolar potencies against HIV-1 in cell culture and low nanomolar biochemical inhibition against INST. Molecular modeling showed that the representative inhibitor **45** binds to IN with a mode similar to **3**. Antiviral testing of **45** against a panel of raltegravir-resistant HIV-1 clones showed a resistance profile similar to that of **3**. However, analogues of our new chemotype also potently inhibited the RNase H function of RT, suggesting that the antiviral potency could be due to dual target inhibition. *in vitro* ADME assays also demonstrated largely favorable physicochemical properties for the new chemotype.

Experimental

Chemistry

1
2
3 **General Procedures.** All commercial chemicals were used as supplied unless otherwise
4 indicated. Dry solvents were either purchased (dioxane and MeOH) or dispensed under
5 argon from an anhydrous solvent system with two packed columns of neutral alumina or
6 molecular sieves. Flash chromatography was performed on a Teledyne Combiflash RF-
7 200 with RediSep columns (silica) and indicated mobile phase. All moisture sensitive
8 reactions were performed under an inert atmosphere of ultra-pure argon with oven-dried
9 glassware. ^1H and ^{13}C NMR spectra were recorded on a Varian 600 MHz spectrometer.
10 Mass data were acquired on an Agilent TOF II TOS/MS spectrometer capable of ESI and
11 APCI ion sources. Analysis of sample purity was performed on a Varian Prepstar SD-1
12 HPLC system with a Phenomenex Gemini, 5 micron C18 column (250mm x 4.6 mm).
13 HPLC conditions: solvent A = H_2O containing 0.1% TFA, solvent B = MeCN; flow rate =
14 1.0 mL/min; compounds were eluted with a gradient of 20% MeCN/ H_2O to 100% MeCN
15 for 30 min. Purity was determined by total absorbance at 254 nm. All tested compounds
16 have a purity $\geq 96\%$.
17
18
19
20
21
22
23
24
25
26
27
28
29
30
31
32
33
34
35

36
37 **General method of 3-*O*-benzyl deprotection for the synthesis of final compounds 24–**
38
39 **55.**

40
41 **Method A: catalytic hydrogenation.** To a solution of 100 mg of 3-(benzyloxy)-
42 pyrimidine-2,4(1H,3H)-dione intermediate (**10, 12, 14–16, 20**) in 7.0 mL MeOH was added
43 20 mg Pearlman's catalyst (Pd-C, 20%). The reaction mixture was degassed using vacuum
44 and refilling with H_2 (40-50 psi) for three times. Then keep the reaction mixture being
45 shaken under H_2 (40-50 psi) atmosphere for appropriate time. The reaction was monitored
46 by both TLC and LC-MS. The reaction mixture was filtered through a short celite column
47
48
49
50
51
52
53
54
55
56
57
58
59
60

1
2
3 and then removed the solvent. Trituration with MeOH, ethyl acetate and DCM provided
4
5
6 desired final compounds **24–55** in 82–97% yield.

7
8 **Method B: acid hydrolysis.** To a microwave reaction vessel were added 0.26 mmol of a
9
10 3-(benzyloxy)-pyrimidine-2,4(1H,3H)-dione intermediate (**10**, **12**, **14–16**, **20**) and 6~10
11
12 mL of TFA. The reaction vessel was irradiated at 120 °C for the appropriate time. The
13
14 reaction was monitored by both TLC and LC-MS. The reaction mixture was transferred to
15
16 a round-bottom flask to remove the solvent under reduced pressure. Then the residue was
17
18 purified by flash chromatography on C18 reverse phase column (H₂O-MeOH) or trituration
19
20 (MeOH, Ethylacetate and DCM) to provide the desired compounds **24–55** as solid in 50-
21
22
23
24
25
26
27 77%.

28 **N-Benzyl-1-(hydroxy)-1,2,3,6-tetrahydro-2,6-dioxo-4-(phenylamino)pyrimidine-5-**
29
30 **carboxamide (24).** White solid, 50% yield; ¹H NMR (600 MHz, DMSO-*d*₆): δ 12.72 (s,
31
32 1H), 11.26 (s, 1H), 10.32 (s, 1H), 10.03 (t, *J* = 2.4, 1H), 7.43-7.26 (m, 10H), 4.49 (s, 2H);
33
34 ¹³C NMR (150 MHz, DMSO-*d*₆): δ 167.7, 161.6, 154.0, 147.0, 139.3, 135.8, 129.5, 128.4,
35
36 127.2, 126.9, 126.5, 124.9, 81.7, 41.9; HRMS-ESI(-) *m/z* calcd for C₁₈H₁₆N₄O₄ 351.1099
37
38 [M-H]⁻, found 351.1103.

39
40
41
42 **N-Benzyl-1-(hydroxy)-1,2,3,6-tetrahydro-2,6-dioxo-4-(biphenylamino)pyrimidine-5-**
43
44 **carboxamide (25).** White solid, 77% yield; ¹H NMR (600 MHz, DMSO-*d*₆): δ 12.76 (s,
45
46 1H), 11.33 (s, 1H), 10.34 (s, 1H), 10.04 (dd, *J* = 6.0, 4.8 1H), 7.74-7.20 (m, 14H), 4.50 (d,
47
48 *J* = 5.4, 2H); ¹³C NMR (150 MHz, DMSO-*d*₆): δ 167.7, 161.6, 154.0, 147.0, 139.3, 138.1,
49
50 135.2, 129.0, 128.4, 127.7, 127.5, 127.2, 126.9, 126.5, 125.4, 80.9, 41.9; HRMS-ESI(-)
51
52
53
54
55
56
57
58
59
60 *m/z* calcd for C₂₄H₂₀N₄O₄ 427.1412 [M-H]⁻, found 427.1414.

1
2
3
4 **N-Benzyl-1-(hydroxy)-1,2,3,6-tetrahydro-4-(methylamino)-2,6-dioxypyrimidine-5-**
5 **carboxamide (26).** White solid, 39% yield; ^1H NMR (600 MHz, DMSO-*d*6): δ 11.05 (s,
6 1H), 10.88 (q, $J = 4.8$ Hz, 1H), 10.20 (s, 1H), 9.90 (t, $J = 6.0$ Hz, 1H), 7.33-7.22 (m, 5H),
7 4.43 (d, $J = 6.0$ Hz, 2H); 2.94 (d, $J = 5.4$ Hz, 3H); ^{13}C NMR (150 MHz, DMSO-*d*6): δ
8 167.7, 161.3, 155.7, 147.3, 139.7, 128.3, 127.1, 126.7, 79.0, 41.7, 28.4; HRMS-ESI(-) m/z
9 calcd for $\text{C}_{13}\text{H}_{14}\text{N}_4\text{O}_4$ 289.0942 $[\text{M}-\text{H}]^-$, found 289.0939.

10
11
12
13
14
15
16
17
18 **N-(3-Fluorobenzyl)-1-(hydroxy)-1,2,3,6-tetrahydro-4-(methylamino)-2,6-**
19 **dioxypyrimidine-5-carboxamide (27).** White solid, 20% yield; ^1H NMR (600 MHz,
20 DMSO-*d*6): δ 11.05 (s, 1H), 10.80 (q, $J = 4.8$ Hz, 1H), 10.18 (s, 1H), 9.94 (t, $J = 6.0$ Hz,
21 1H), 7.35 (ddd, $J = 7.8, 7.2, 6.0$ Hz, 1H), 7.11 (d, $J = 7.2$ Hz, 1H), 7.06 (m, 2H), 4.44 (d, J
22 = 6.0 Hz, 2H); 2.93 (d, $J = 4.2$ Hz, 3H); ^{13}C NMR (150 MHz, DMSO-*d*6): δ 167.8, 162.2
23 (d, $J_{\text{CF}} = 241.5$ Hz), 161.3, 155.9, 147.4, 143.0 (d, $J_{\text{CF}} = 6.9$ Hz), 130.2 (d, $J_{\text{CF}} = 8.1$ Hz),
24 123.1 (d, $J_{\text{CF}} = 2.4$ Hz), 113.7 (d, $J_{\text{CF}} = 21.9$ Hz), 113.4 (d, $J_{\text{CF}} = 20.0$ Hz), 79.0, 41.2, 28.4;
25 HRMS-ESI(-) m/z calcd for $\text{C}_{13}\text{H}_{13}\text{FN}_4\text{O}_4$ 307.0848 $[\text{M}-\text{H}]^-$, found 307.0852.

26
27
28
29
30
31
32
33
34
35
36
37
38 **N-(4-Fluorobenzyl)-1-(hydroxy)-1,2,3,6-tetrahydro-4-(methylamino)-2,6-**
39 **dioxypyrimidine-5-carboxamide (28).** White solid, 20% yield; ^1H NMR (600 MHz,
40 DMSO-*d*6): δ 11.05 (s, 1H), 10.86 (q, $J = 5.4$ Hz, 1H), 10.19 (s, 1H), 9.87 (t, $J = 6.0$ Hz,
41 1H), 7.31 (dd, $J = 8.4, 5.4$ Hz, 2H), 7.14 (t, $J = 9.0$ Hz, 2H), 4.41 (d, $J = 5.4$ Hz, 2H); 2.94
42 (d, $J = 4.8$ Hz, 3H); ^{13}C NMR (150 MHz, DMSO-*d*6): δ 167.7, 163.7, 161.1 (d, $J_{\text{CF}} = 241.5$
43 Hz), 161.2, 155.7, 147.3, 136.0 (d, $J_{\text{CF}} = 2.4$ Hz), 129.1 (d, $J_{\text{CF}} = 8.1$ Hz), 115.0 (d, $J_{\text{CF}} =$
44 20.7 Hz), 79.0, 40.9, 28.4; HRMS-ESI(-) m/z calcd for $\text{C}_{13}\text{H}_{13}\text{FN}_4\text{O}_4$ 307.0848 $[\text{M}-\text{H}]^-$,
45 found 307.0850.

1
2
3
4
5
6
7
8
9
10
11
12
13
14
15
16
17
18
19
20
21
22
23
24
25
26
27
28
29
30
31
32
33
34
35
36
37
38
39
40
41
42
43
44
45
46
47
48
49
50
51
52
53
54
55
56
57
58
59
60

N-(3-Chloro-2-fluorobenzyl)-1-(hydroxy)-1,2,3,6-tetrahydro-4-(methylamino)-2,6-dioxypyrimidine-5-carboxamide (29). White solid, 90 % yield; ^1H NMR (600 MHz, DMSO-*d*6): δ 11.06 (s, 1H), 10.76 (q, $J = 4.2$ Hz, 1H), 10.22 (s, 1H), 9.95 (t, $J = 6.0$ Hz, 1H), 7.47 (t, $J = 7.2$ Hz, 1H), 7.27 (dd, $J = 7.8, 6.0$ Hz, 1H), 7.18 (t, $J = 7.8$ Hz, 1H), 4.50 (d, $J = 4.8$ Hz, 2H), 2.93 (d, $J = 4.2$ Hz, 3H); ^{13}C NMR (150 MHz, DMSO-*d*6): δ 167.8, 161.3, 155.7, 155.2 (d, $J_{\text{CF}} = 246$ Hz), 147.3, 129.0, 128.7 (d, $J_{\text{CF}} = 13.8$ Hz), 128.2 (d, $J_{\text{CF}} = 4.5$ Hz), 125.2 (d, $J_{\text{CF}} = 4.7$ Hz), 119.4 (d, $J_{\text{CF}} = 17.3$ Hz), 79.0, 35.9 (d, $J_{\text{CF}} = 3.5$ Hz), 28.4; HRMS-ESI(-) m/z calcd for $\text{C}_{13}\text{H}_{12}\text{ClFN}_4\text{O}_4$ 341.0458 [M-H] $^-$, found 341.0462.

N-Benzyl-1-(hydroxy)-4-(ethylamino)-1,2,3,6-tetrahydro-2,6-dioxypyrimidine-5-carboxamide (30). White solid, 42% yield; ^1H NMR (600 MHz, DMSO-*d*6): δ 11.11 (s, 1H), 11.04 (t, $J = 5.4$ Hz, 1H), 10.20 (s, 1H), 9.93 (t, $J = 6.0$ Hz, 1H), 7.34-7.24 (m, 5H), 4.43 (d, $J = 6.0$ Hz, 2H); 3.36 (td, $J = 6.6, 6.0$ Hz, 2H), 1.14 (t, $J = 6.6$ Hz, 3H); ^{13}C NMR (150 MHz, DMSO-*d*6): δ 167.8, 161.4, 154.7, 147.3, 139.6, 128.4, 127.1, 126.8, 78.8, 41.7, 36.0, 14.4; HRMS-ESI(-) m/z calcd for $\text{C}_{14}\text{H}_{16}\text{N}_4\text{O}_4$ 303.1099 [M-H] $^-$, found 303.1098.

N-Benzyl-1-(hydroxy)-1,2,3,6-tetrahydro-2,6-dioxo-4-(propylamino)pyrimidine-5-carboxamide (31). White solid, 79% yield; ^1H NMR (600 MHz, DMSO-*d*6): δ 11.16 (s, 1H), 11.13 (s, 1H), 10.20 (s, 1H), 9.94 (s, 1H), 7.32-7.24 (m, 5H), 4.44 (d, $J = 4.8$ Hz, 2H); 3.30 (m, 2H), 1.54 (m, 2H), 0.91 (t, $J = 6.6$ Hz, 3H); ^{13}C NMR (150 MHz, DMSO-*d*6): δ 167.9, 161.4, 154.9, 147.3, 139.6, 128.4, 127.1, 126.8, 78.8, 42.6, 41.7, 22.1, 11.0; HRMS-ESI(-) m/z calcd for $\text{C}_{15}\text{H}_{18}\text{N}_4\text{O}_4$ 317.1255 [M-H] $^-$, found 317.1253.

N-(3-Chloro-2-fluorobenzyl)-1-(hydroxy)-1,2,3,6-tetrahydro-2,6-dioxo-4-(propylamino)pyrimidine-5-carboxamide (32). White solid, 73 % yield; ^1H NMR (600

MHz, DMSO-*d*₆): δ 11.15 (s, 1H), 11.02 (s, 1H), 10.23 (s, 1H), 9.99 (s, 1H), 7.47-7.18 (m, 3H), 4.51 (d, *J* = 4.2 Hz, 2H), 3.30 (m, 2H), 1.52 (m, 2H), 0.89 (dd, *J* = 7.8, 6.0 Hz, 3H); ¹³C NMR (150 MHz, DMSO-*d*₆): δ 168.0, 161.4, 155.2 (d, *J*_{CF} = 246 Hz), 154.9, 147.3, 129.1, 128.6 (d, *J*_{CF} = 14.9 Hz), 128.2 (d, *J*_{CF} = 4.5 Hz), 125.3 (d, *J*_{CF} = 3.5 Hz), 119.5 (d, *J*_{CF} = 17.3 Hz), 78.8, 42.6, 35.9 (d, *J*_{CF} = 3.5 Hz), 22.0, 11.0; HRMS-ESI(-) *m/z* calcd for C₁₅H₁₆ClFN₄O₄ 369.0771 [M-H]⁻, found 369.0768.

N-Benzyl-1-(hydroxy)-1,2,3,6-tetrahydro-4-(isopropylamino)-2,6-dioxypyrimidine-5-carboxamide (33). White solid, 92% yield; ¹H NMR (600 MHz, DMSO-*d*₆): δ 11.18 (d, *J* = 8.4 Hz 1H), 11.14 (s, 1H), 10.21 (s, 1H), 9.96 (d, *J* = 5.4 Hz 1H), 7.34-7.23 (m, 5H), 4.43 (d, *J* = 5.4 Hz, 2H); 4.08 (m, 1H), 1.16 (d, *J* = 6.0 Hz, 6H); ¹³C NMR (150 MHz, DMSO-*d*₆): δ 167.9, 161.4, 153.8, 147.3, 139.6, 128.4, 127.1, 126.8, 78.7, 42.6, 41.7, 22.8; HRMS-ESI(-) *m/z* calcd for C₁₅H₁₈N₄O₄ 317.1255 [M-H]⁻, found 317.1261.

N-Benzyl-1-(hydroxy)-4-(cyclopropylamino)-1,2,3,6-tetrahydro-2,6-dioxypyrimidine-5-carboxamide (34). White solid, 82% yield; ¹H NMR (600 MHz, DMSO-*d*₆): δ 11.17 (s, 1 H), 11.01 (s, 1H), 10.24 (s, 1H), 9.87 (t, *J* = 6.0 Hz 1H), 7.31-7.21 (m, 5H), 4.39 (d, *J* = 5.4 Hz, 2H); 2.71 (m, 1H), 0.83 (m, 2H), 0.59 (m, 2 H); ¹³C NMR (150 MHz, DMSO-*d*₆): δ 167.6, 161.2, 156.5, 147.1, 139.5, 128.4, 127.1, 126.8, 79.2, 41.7, 23.0, 7.7; HRMS-ESI(-) *m/z* calcd for C₁₅H₁₆N₄O₄ 315.1099 [M-H]⁻, found 315.1101.

4-(Tert-butylamino)-N-benzyl-1-(hydroxy)-1,2,3,6-tetrahydro-2,6-dioxypyrimidine-5-carboxamide (35). White solid, 59% yield; ¹H NMR (600 MHz, DMSO-*d*₆): δ 11.82 (s, 1H), 10.24 (s, 1H), 10.10 (t, *J* = 6.0 Hz, 1H), 10.03 (brs, 1H), 7.33-7.25 (m, 5H), 4.43 (d,

1
2
3
4
5
6
7
8
9
10
11
12
13
14
15
16
17
18
19
20
21
22
23
24
25
26
27
28
29
30
31
32
33
34
35
36
37
38
39
40
41
42
43
44
45
46
47
48
49
50
51
52
53
54
55
56
57
58
59
60

$J = 5.4$ Hz, 2H), 1.41 (s, 9H); ^{13}C NMR (150 MHz, DMSO-*d*6): δ 168.1, 161.4, 153.7, 146.8, 139.5, 128.4, 127.1, 126.8, 78.9, 52.0, 41.7, 29.0; HRMS-ESI(-) m/z calcd for $\text{C}_{16}\text{H}_{20}\text{N}_4\text{O}_4$ 331.1412 [M-H] $^-$, found 331.1416.

4-Amino-N-benzyl-1-(hydroxy)-1,2,3,6-tetrahydro-2,6-dioxypyrimidine-5-

carboxamide (46). White solid, 89% yield; ^1H NMR (600 MHz, DMSO-*d*6): δ 11.19 (brs, 1H), 10.13 (brs, 1H), 9.78 (s, 1H), 9.68 (s, 1H), 7.32-7.24 (m, 4H), 6.88 (brs, 1H), 4.43 (d, $J = 4.8$ Hz, 2H); ^{13}C NMR (150 MHz, DMSO-*d*6): δ 167.1, 161.8, 156.4, 147.5, 139.7, 128.3, 127.1, 126.7, 79.8, 41.6; HRMS-ESI(-) m/z calcd for $\text{C}_{12}\text{H}_{12}\text{N}_4\text{O}_4$ 275.0786 [M-H] $^-$, found 275.0785.

N-(3-Fluorobenzyl)-1-(hydroxy)-4-(ethylamino)-1,2,3,6-tetrahydro-2,6-

dioxypyrimidine-5-carboxamide (47). White solid, 76% yield; ^1H NMR (600 MHz, DMSO-*d*6): δ 11.11 (s, 1H), 11.98 (t, $J = 4.8$ Hz, 1H), 10.22 (s, 1H), 9.97 (t, $J = 6.0$ Hz, 1H), 7.36 (q, 7.2 Hz, 1H), 7.11 (d, $J = 7.2$ Hz, 1H), 7.06 (m, 2H), 4.45 (d, $J = 6.0$ Hz, 2H); 3.36 (td, $J = 7.2, 6.6$ Hz, 2H), 1.14 (t, $J = 7.2$ Hz, 3H); ^{13}C NMR (150 MHz, DMSO-*d*6): δ 167.9, 161.5 (d, $J_{\text{CF}} = 241.5$ Hz), 161.4, 154.7, 147.3, 142.9 (d, $J_{\text{CF}} = 6.9$ Hz), 130.3 (d, $J_{\text{CF}} = 8.0$ Hz), 123.0, 113.7 (d, $J_{\text{CF}} = 21.8$ Hz), 113.5 (d, $J_{\text{CF}} = 20.7$ Hz), 78.8, 41.2, 36.1, 14.4; HRMS-ESI(-) m/z calcd for $\text{C}_{14}\text{H}_{15}\text{FN}_4\text{O}_4$ 321.1005 [M-H] $^-$, found 321.1005.

N-(4-Fluorobenzyl)-1-(hydroxy)-4-(ethylamino)-1,2,3,6-tetrahydro-2,6-

dioxypyrimidine-5-carboxamide (38). White solid, 33% yield; ^1H NMR (600 MHz, DMSO-*d*6): δ 11.10 (s, 1H), 11.01 (t, $J = 5.4$ Hz, 1H), 10.20 (s, 1H), 9.93 (t, $J = 6.0$ Hz, 1H), 7.31 (dd, $J = 8.4, 5.4$ Hz, 2H), 7.14 (t, $J = 9.0$ Hz, 2H), 4.41 (d, $J = 5.4$ Hz, 2H), 3.36 (td, $J = 7.2, 6.6$ Hz, 2H), 1.14 (t, $J = 7.2$ Hz, 3H); ^{13}C NMR (150 MHz, DMSO-*d*6): δ

1
2
3 167.8, 161.3, 161.1 (d, J_{CF} = 240.3 Hz), 154.7, 147.3, 135.9 (d, J_{CF} = 2.3 Hz), 129.1 (d, J_{CF}
4 = 8.0 Hz), 115.0 (d, J_{CF} = 21.9 Hz), 78.8, 40.9, 36.0, 14.4; HRMS-ESI(-) m/z calcd for
5
6 $C_{14}H_{15}FN_4O_4$ 321.1005 [M-H]⁻, found 321.1003.
7
8

9
10
11 **N-(2,5-difluorobenzyl)-1-(hydroxy)-4-(ethylamino)-1,2,3,6-tetrahydro-2,6-**
12

13 **dioxypyrimidine-5-carboxamide (39).** White solid, 32% yield; ¹H NMR (600 MHz,
14 DMSO-*d*₆): δ 11.12 (s, 1H), 11.90 (t, J = 5.4 Hz, 1H), 10.23 (s, 1H), 9.96 (t, J = 6.0 Hz,
15 1H), 7.25-7.07 (m, 3H), 4.45 (d, J = 5.4 Hz, 2H); 3.36 (td, J = 7.2, 6.6 Hz, 2H), 1.13 (t, J
16 = 7.2 Hz, 3H); HRMS-ESI(-) m/z calcd for $C_{14}H_{14}F_2N_4O_4$ 339.091 [M-H]⁻, found
17
18 339.0911.
19
20
21
22
23

24
25
26 **N-(2,4-difluorobenzyl)-1-(hydroxy)-4-(ethylamino)-1,2,3,6-tetrahydro-2,6-**
27

28 **dioxypyrimidine-5-carboxamide (40).** White solid, 26% yield; ¹H NMR (600 MHz,
29 DMSO-*d*₆): δ 11.11 (s, 1H), 10.91 (t, J = 5.4 Hz, 1H), 10.19 (s, 1H), 9.94 (t, J = 6.0 Hz,
30 1H), 7.36-7.04 (m, 3H), 4.43 (d, J = 6.0 Hz, 2H); 3.35 (td, J = 7.2, 6.6 Hz, 2H), 1.13 (t, J
31 = 7.2 Hz, 3H); HRMS-ESI(-) m/z calcd for $C_{14}H_{14}F_2N_4O_4$ 339.091 [M-H]⁻, found
32
33 339.0915.
34
35
36
37
38
39

40
41 **N-(3,5-difluorobenzyl)-1-(hydroxy)-4-(ethylamino)-1,2,3,6-tetrahydro-2,6-**
42

43 **dioxypyrimidine-5-carboxamide (41).** White solid, 61% yield; ¹H NMR (600 MHz,
44 DMSO-*d*₆): δ 11.12 (s, 1H), 10.92 (s, 1H), 10.23 (s, 1H), 9.99 (t, J = 5.4 Hz, 1H), 7.09-
45 6.96 (m, 3H), 4.45 (d, J = 5.4 Hz, 2H); 3.36 (m, 2H), 1.14 (dd, J = 7.2, 6.6 Hz, 3H);
46
47 HRMS-ESI(-) m/z calcd for $C_{14}H_{14}F_2N_4O_4$ 339.091 [M-H]⁻, found 339.0914.
48
49
50

51
52
53 **N-(3,4-difluorobenzyl)-1-(hydroxy)-4-(ethylamino)-1,2,3,6-tetrahydro-2,6-**
54

55 **dioxypyrimidine-5-carboxamide (42).** White solid, 56% yield; ¹H NMR (600 MHz,
56
57
58
59
60

1
2
3
4
5
6
7
8
9
10
11
12
13
14
15
16
17
18
19
20
21
22
23
24
25
26
27
28
29
30
31
32
33
34
35
36
37
38
39
40
41
42
43
44
45
46
47
48
49
50
51
52
53
54
55
56
57
58
59
60

DMSO-*d*₆): δ 11.11 (s, 1H), 10.96 (s, 1H), 10.21 (s, 1H), 9.96 (s, 1H), 7.38-7.16 (m, 3H), 4.41 (d, $J = 3.6$ Hz, 2H); 3.36 (m, 2H), 1.14 (dd, $J = 7.2, 4.8$ Hz, 3H); HRMS-ESI(-) m/z calcd for C₁₄H₁₄F₂N₄O₄ 339.091 [M-H]⁻, found 339.0915.

N-(2-Chloro-5-fluorobenzyl)-1-(hydroxy)-4-(ethylamino)-1,2,3,6-tetrahydro-2,6-

dioxypyrimidine-5-carboxamide (43). White solid, 20 % yield; ¹H NMR (600 MHz, DMSO-*d*₆): δ 11.13 (s, 1H), 10.88 (dd, $J = 5.4, 4.2$ Hz, 1H), 10.24 (s, 1H), 10.03 (t, $J = 6.0$ Hz, 1H), 7.50 (dd, $J = 9.0, 5.4$ Hz, 1H), 7.16 (td, $J = 8.4, 3.0$ Hz, 1H), 7.09 (dd, $J = 9.6, 2.4$ Hz, 1H), 4.47 (d, $J = 6.0$ Hz, 2H), 3.35 (td, $J = 7.2, 6.6$ Hz, 2H), 1.13 (t, $J = 7.2$ Hz, 3H); ¹³C NMR (150 MHz, DMSO-*d*₆): δ 168.0, 161.4, 160.8 (d, $J_{CF} = 242.7$ Hz), 154.7, 147.3, 139.5 (d, $J_{CF} = 6.9$ Hz), 130.9 (d, $J_{CF} = 8.1$ Hz), 127.2 (d, $J_{CF} = 2.3$ Hz), 116.2 (d, $J_{CF} = 24.2$ Hz), 115.4 (d, $J_{CF} = 23.1$ Hz), 78.8, 39.8, 36.1, 14.3; HRMS-ESI(-) m/z calcd for C₁₄H₁₄ClFN₄O₄ 355.0615 [M-H]⁻, found 355.0618.

N-(4-Chloro-3-fluorobenzyl)-1-(hydroxy)-4-(ethylamino)-1,2,3,6-tetrahydro-2,6-

dioxypyrimidine-5-carboxamide (44). White solid, 51 % yield; ¹H NMR (600 MHz, DMSO-*d*₆): δ 11.12 (s, 1H), 10.94 (t, $J = 5.4$ Hz, 1H), 10.22 (s, 1H), 9.98 (t, $J = 6.0$ Hz, 1H), 7.53 (dd, $J = 8.4, 7.2$ Hz, 1H), 7.28 (d, $J = 10.8$ Hz, 1H), 7.19 (d, $J = 8.4$ Hz, 1H), 4.43 (d, $J = 6.0$ Hz, 2H), 3.36 (td, $J = 7.2, 6.6$ Hz, 2H), 1.13 (t, $J = 7.2$ Hz, 3H); ¹³C NMR (150 MHz, DMSO-*d*₆): δ 168.0, 161.3, 157.0 (d, $J_{CF} = 244.8$ Hz), 154.7, 147.3, 142.0 (d, $J_{CF} = 5.7$ Hz), 130.4, 124.2 (d, $J_{CF} = 3.4$ Hz), 117.4 (d, $J_{CF} = 17.3$ Hz), 115.4 (d, $J_{CF} = 20.7$ Hz), 78.8, 40.8, 36.1, 14.3; HRMS-ESI(-) m/z calcd for C₁₄H₁₄ClFN₄O₄ 355.0615 [M-H]⁻, found 355.0621.

1
2
3
4
5
6
7
8
9
10
11
12
13
14
15
16
17
18
19
20
21
22
23
24
25
26
27
28
29
30
31
32
33
34
35
36
37
38
39
40
41
42
43
44
45
46
47
48
49
50
51
52
53
54
55
56
57
58
59
60

N-(3-Chloro-2-fluorobenzyl)-1-(hydroxy)-4-(ethylamino)-1,2,3,6-tetrahydro-2,6-dioxypyrimidine-5-carboxamide (45). White solid, 90 % yield; ^1H NMR (600 MHz, DMSO-*d*6): δ 11.12 (s, 1H), 10.90 (t, $J = 5.4$ Hz, 1H), 10.23 (s, 1H), 9.99 (t, $J = 6.0$ Hz, 1H), 7.48 (t, $J = 7.2$ Hz, 1H), 7.27 (dd, $J = 7.2$ Hz, 1H), 7.19 (t, $J = 7.8$ Hz, 1H), 4.50 (d, $J = 4.2$ Hz, 2H), 3.35 (td, $J = 7.2, 6.6$ Hz, 2H), 1.13 (t, $J = 7.2$ Hz, 3H); ^{13}C NMR (150 MHz, DMSO-*d*6): δ 167.9, 161.4, 155.2 (d, $J_{\text{CF}} = 244.8$ Hz), 154.7, 147.3, 129.1, 128.6 (d, $J_{\text{CF}} = 13.8$ Hz), 128.2 (d, $J_{\text{CF}} = 3.5$ Hz), 125.2 (d, $J_{\text{CF}} = 4.5$ Hz), 119.4 (d, $J_{\text{CF}} = 17.3$ Hz), 78.8, 36.0, 35.9 (d, $J_{\text{CF}} = 3.5$ Hz), 14.4; HRMS-ESI(-) m/z calcd for $\text{C}_{14}\text{H}_{14}\text{ClFN}_4\text{O}_4$ 355.0615 [M-H] $^-$, found 355.0620.

N-(3-Fluoro-4-methylbenzyl)-1-(hydroxy)-4-(ethylamino)-1,2,3,6-tetrahydro-2,6-dioxypyrimidine-5-carboxamide (46). White solid, 37 % yield; ^1H NMR (600 MHz, DMSO-*d*6): δ 11.11 (s, 1H), 11.00 (t, $J = 5.4$ Hz, 1H), 10.21 (s, 1H), 9.93 (t, $J = 5.4$ Hz, 1H), 7.22 (t, $J = 7.8$ Hz, 1H), 7.01 (m, 2H), 4.39 (d, $J = 6.0$ Hz, 2H), 3.36 (td, $J = 6.6, 6.0$ Hz, 2H), 2.19 (s, 3H), 1.13 (dd, $J = 7.2, 6.6$ Hz, 3H); ^{13}C NMR (150 MHz, DMSO-*d*6): δ 167.9, 161.4, 160.5 (d, $J_{\text{CF}} = 239.3$ Hz), 154.7, 147.3, 139.9 (d, $J_{\text{CF}} = 6.9$ Hz), 131.5 (d, $J_{\text{CF}} = 5.7$ Hz), 122.8 (d, $J_{\text{CF}} = 3.5$ Hz), 122.3 (d, $J_{\text{CF}} = 17.3$ Hz), 113.5 (d, $J_{\text{CF}} = 21.8$ Hz), 78.8, 41.0, 36.0, 14.4, 13.8 (d, $J_{\text{CF}} = 3.5$ Hz); HRMS-ESI(-) m/z calcd for $\text{C}_{15}\text{H}_{17}\text{FN}_4\text{O}_4$ 335.1161 [M-H] $^-$, found 335.1164.

1-(Hydroxy)-4-(ethylamino)-1,2,3,6-tetrahydro-2,6-dioxo-N-phenethylpyrimidine-5-carboxamide (47). White solid, 79% yield; ^1H NMR (600 MHz, DMSO-*d*6): δ 11.11 (t, $J = 5.4$ Hz, 1H), 11.06 (s, 1H), 10.17 (s, 1H), 9.56 (t, $J = 5.4$ Hz, 1H), 7.30-7.19 (m, 5H), 3.45 (ddd, $J = 7.2, 6.6, 6.0$ Hz, 2H); 3.35 (qd, $J = 7.2, 6.6$ Hz, 2H), 2.77 (t, $J = 7.2$ Hz, 3H), 1.14 (t, $J = 7.2$ Hz, 3H); ^{13}C NMR (150 MHz, DMSO-*d*6): δ 167.8, 161.2, 154.6,

1
2
3
4
5
6
7
8
9
10
11
12
13
14
15
16
17
18
19
20
21
22
23
24
25
26
27
28
29
30
31
32
33
34
35
36
37
38
39
40
41
42
43
44
45
46
47
48
49
50
51
52
53
54
55
56
57
58
59
60

147.3, 139.4, 128.6, 128.4, 126.1, 78.9, 39.8, 36.0, 35.3, 14.4; HRMS-ESI(-) m/z calcd for $C_{15}H_{18}N_4O_4$ 317.1255 [M-H]⁻, found 317.1257.

1-(Hydroxy)-4-(ethylamino)-1,2,3,6-tetrahydro-2,6-dioxo-N-phenylpyrimidine-5-carboxamide (48). White solid, 83% yield; ¹H NMR (600 MHz, DMSO-*d*6): δ 11.89 (s, 1H), 11.26 (s, 1H), 10.89 (t, *J* = 5.4 Hz, 1H), 10.38 (s, 1H), 7.55 (d, *J* = 7.8 Hz, 2H), 7.31 (dd, *J* = 7.8, 7.2 Hz, 2H), 7.31 (dd, *J* = 7.8, 7.2 Hz, 1H), 3.42 (qd, *J* = 6.6, 6.0 Hz, 2H), 1.18 (t, *J* = 6.6 Hz, 3H); ¹³C NMR (150 MHz, DMSO-*d*6): δ 166.3, 161.8, 154.9, 147.1, 138.5, 128.9, 123.1, 119.8, 79.2, 36.3, 14.4; HRMS-ESI(-) m/z calcd for $C_{13}H_{14}N_4O_4$ 289.0942 [M-H]⁻, found 289.0942.

1-(Hydroxy)-1,2,3,6-tetrahydro-2,6-dioxo-4-(phenylamino)pyrimidine-5-carboxamide (49). White solid; ¹H NMR (600 MHz, DMSO-*d*6): δ 12.90 (s, 1H), 11.20 (s, 1H), 10.27 (s, 1H), 8.96 (s, 1H), 7.44–7.27 (m, 5H); ¹³C NMR (150 MHz, DMSO-*d*6): δ 169.9, 161.4, 154.2, 147.0, 135.8, 129.6, 126.4, 124.9, 80.7; HRMS-ESI(-) m/z calcd for $C_{11}H_{10}N_4O_4$ 261.0629 [M-H]⁻, found 261.0632.

1-(Hydroxy)-N-(2-chloroethyl)-4-(ethylamino)-1,2,3,6-tetrahydro-2,6-dioxypyrimidine-5-carboxamide (50). White solid, 83% yield; ¹H NMR (600 MHz, DMSO-*d*6): δ 11.11 (s, 1H), 11.98 (s, 1H), 10.22 (s, 1H), 9.78 (s, 1H), 3.68 (m, 2H), 3.55 (m, 2H), 3.37 (m, 2H), 1.15 (t, *J* = 6.6 Hz, 3H); ¹³C NMR (150 MHz, DMSO-*d*6): δ 168.0, 161.2, 154.7, 147.3, 78.7, 43.97, 40.1, 36.1, 14.4; HRMS-ESI(-) m/z calcd for $C_9H_{13}ClN_4O_4$ 275.0553 [M-H]⁻, found 275.0552.

Phenyl-1-(hydroxy)-4-(ethylamino)-1,2,3,6-tetrahydro-2,6-dioxypyrimidine-5-carboxylate (51). White solid, 92% yield; ¹H NMR (600 MHz, DMSO-*d*6): δ 11.16 (s,

1
2
3 1H), 10.12 (s, 1H), 9.49 (s, 1H), 7.41-7.09 (m, 5H), 3.42 (m, 2H), 1.14 (m, 3H); ¹³C NMR
4
5 (150 MHz, DMSO-*d*6): δ 167.2, 157.2, 155.6, 150.7, 147.6, 129.3, 125.3, 122.1, 78.2, 36.5,
6
7 14.2; HRMS-ESI(-) *m/z* calcd for C₁₃H₁₃N₃O₅ 290.0782 [M-H]⁻, found 290.0784.

8
9
10
11 **N-(4-Fluorobenzyl)-3-(hydroxy)-6-(ethylamino)-1,2,3,4-tetrahydro-1-methyl-2,4-**
12 **dioxopyrimidine-5-carboxamide (52).** White solid, 38% yield; ¹H NMR (600 MHz,
13
14 DMSO-*d*6): δ 11.89 (s, 1H), 10.29 (s, 1H), 9.93 (s, 1H), 7.32 (m, 2H), 7.14 (m, 2H), 4.43
15
16 (d, *J* = 4.2 Hz, 2H), 4.00 (s, 3H), 3.47 (m, 2H), 1.16 (dd, *J* = 6.6, 5.4 Hz, 3H); ¹³C NMR
17
18 (150 MHz, DMSO-*d*6): δ 167.6, 161.1 (d, *J*_{CF} = 240.3 Hz), 160.5, 159.8, 154.2, 135.9,
19
20 129.1 (d, *J*_{CF} = 8.1 Hz), 115.0 (d, *J*_{CF} = 20.7 Hz), 84.4, 55.6, 41.0, 35.2, 14.8; HRMS-ESI(-)
21
22) *m/z* calcd for C₁₅H₁₇FN₄O₄ 335.1161 [M-H]⁻, found 335.1158.

23
24
25
26
27
28
29 **3-(Benzyloxy)-6-(ethylamino)-N-(4-fluorobenzyl)-N-methyl-2,4-dioxo-1,2,3,4-**
30 **tetrahydropyrimidine-5-carboxamide (53).** White solid, 28% yield; ¹H NMR (600 MHz,
31
32 DMSO-*d*6): δ 11.25 (s, 1H), 9.99 (s, 1H), 7.52-7.13 (m, 9H), 4.98 (s, 2H), 4.43 (s, 2H),
33
34 3.43 (m, 2H), 3.38 (s, 3H), 1.19 (dd, *J* = 6.0, 5.4 Hz, 3H); ¹³C NMR (150 MHz, DMSO-
35
36 *d*6): δ 167.5, 161.2 (d, *J*_{CF} = 240.3 Hz), 161.0, 159.9, 148.5, 135.7, 134.4, 129.34, 129.31
37
38 (d, *J*_{CF} = 8.1 Hz), 128.8, 128.3, 115.1 (d, *J*_{CF} = 20.7 Hz), 83.4, 77.3, 41.6, 41.2, 35.9, 15.5;
39
40 HRMS-ESI(-) *m/z* calcd for C₂₂H₂₃FN₄O₄ 425.1631 [M-H]⁻, found 425.1631.

41
42
43
44
45
46 **N-Benzyl-1,6-dihydroxy-2,4-dioxo-1,2,3,4-tetrahydropyrimidine-5-carboxamide**
47
48 **(54).** Pale white solid, 53% yield; ¹H NMR (600 MHz, DMSO-*d*6): δ 11.91 (s, 1H), 10.40
49
50 (s, 1H), 9.97 (s, 1H), 7.36-7.29 (m, 5H), 4.57 (brs, 2H); ¹³C NMR (150 MHz, DMSO-
51
52 *d*6): δ 170.0, 147.6, 137.6, 7, 128.5, 127.41, 127.36, 79.0, 42.8; HRMS-ESI(-) *m/z* calcd
53
54 for C₁₂H₁₁N₃O₅ 276.0626 [M-H]⁻, found 276.0628.
55
56
57
58
59
60

1
2
3 **N-(4-Fluorobenzyl)-7-(hydroxy)-2,3,4,6,7,8-hexahydro-6,8-dioxo-1H-pyrimido[1,6-**
4 **a]pyrimidine-9-carboxamide (55).** Pale white solid, 96 yield; ¹H NMR (600 MHz,
5 DMSO-*d*₆): δ 11.52 (s, 1H), 10.29 (s, 1H), 10.02 (br s, 1H), 7.31-7.13 (m, 4H), 4.42 (d, *J*
6 = 4.8, 2H), 3.82 (m, 2H), 3.38 (m, 2H), 1.94 (m, 2H); ¹³C NMR (150 MHz, DMSO-*d*₆): δ
7 167.9, 161.1 (d, *J*_{CF} = 241.5 Hz), 160.4, 154.1, 147.4, 136.0 (d, *J*_{CF} = 2.3 Hz), 129.1 (d, *J*_{CF}
8 = 8.1 Hz), 115.0 (d, *J*_{CF} = 20.1 Hz), 78.6, 41.0, 40.8, 38.1, 18.8; HRMS-ESI(-) *m/z* calcd
9 for C₁₅H₁₅FN₄O₄ 333.1005 [M-H]⁻, found 333.1001.
10
11
12
13
14
15
16
17
18
19

20 **Biology**

21
22 **INST assay.** HIV integrase was expressed and purified as previously reported.⁵² Inhibition
23 assays were performed using a modified protocol of our reported method.⁵² Briefly, 2.1 μL
24 of compound suspended in DMSO was placed in duplicate into a Black 96 well non-
25 binding plate (corning 3991). Compounds were plated in duplicate to a final concentration
26 of 0.13 — 100 μM. To each well of the plate 186.9 μL of reaction mixture without DNA
27 substrate was added (10 mM HEPES pH 7.5, 10 % glycerol w/v, 10 mM MnCl₂, 1 mM
28 DTT, 1 μM integrase). The enzyme was incubated with inhibitor for 10 min at 25 °C after
29 which the reaction was initiated by the addition of 21 μL of 500 nM oligo (5' biotin
30 ATGTGGAAAATCTCTAGCA annealed with ACTGCTAGAGATTTTCCACAT 3'
31 Cy5). Reactions were incubated at 37 °C for 30 min and then quenched by the addition of
32 5.2 μL 500 mM EDTA. Each reaction was moved (200 μL) to a MultiScreen HTS PCR
33 plate (Millipore MSSLBPC10) containing 20 μL streptavidin agarose beads (Life
34 Technologies S951) and incubated with shaking for 30 min. A vacuum manifold was used
35 to remove the reaction mixture and the beads were similarly washed 3 times with wash
36 buffer (.05% SDS, 1 mM EDTA in PBS). The plates were further washed 3 times with
37
38
39
40
41
42
43
44
45
46
47
48
49
50
51
52
53
54
55
56
57
58
59
60

1
2
3 200 μ L 50 mM NaOH to denature DNA not covalently linked to the biotin modification.
4
5 For each denaturation step the plate was incubated with shaking at 25 °C for 5 min and the
6
7 NaOH was removed by centrifugation at 1000 g for 1 min. The reaction products were
8
9 eluted from the beads by the addition of 150 μ L formamide. The plate was incubated at
10
11 25 °C for 10 min and read directly at 635/675 in a SpectraMax i3 plate reader (Molecular
12
13 Devices).

14
15
16
17
18 Expression and purification of the recombinant IN in *Escherichia coli* were performed as
19
20 previously reported^{39, 53} with addition of 10% glycerol to all buffers. Preparation of
21
22 oligonucleotide substrates has been described.⁵⁴ Integrase reactions were performed in 10
23
24 μ L with 400 nM of recombinant IN, 20 nM of 5'-end [³²P]-labeled oligonucleotide
25
26 substrate and inhibitors at various concentrations. Solutions of 10% DMSO without
27
28 inhibitors were used as controls. Reactions were incubated at 37 °C (60 minutes) in buffer
29
30 containing 50 mM MOPS, pH 7.2, 7.5 mM MgCl₂, and 14.3 mM 2-mercaptoethanol.
31
32 Reactions were stopped by addition of 10 μ L of loading dye (10 mM EDTA, 98%
33
34 deionized formamide, 0.025% xylene cyanol and 0.025% bromophenol blue). Reactions
35
36 were then subjected to electrophoresis in 20% polyacrylamide–7 M urea gels. Gels were
37
38 dried and reaction products were visualized and quantitated with a Typhoon 8600 (GE
39
40 Healthcare, Little Chalfont, Buckinghamshire, UK). Densitometric analyses were
41
42 performed using ImageQuant from Molecular Dynamics Inc. The concentrations at which
43
44 enzyme activity was reduced by 50% (IC₅₀) were determined using “Prism” software
45
46 (GraphPad Software, San Diego, CA) for nonlinear regression to fit dose-response data to
47
48 logistic curve models.
49
50
51
52
53
54
55
56
57
58
59
60

1
2
3 ***RNase H assay.*** RNase H activity was measured essentially as previously described.⁵⁵ Full-
4 length HIV RT was incubated with the RNA/DNA duplex substrate HTS-1 (RNA 5'-
5 gaucugagccugggagcu -3'-fluorescein annealed to DNA 3'-CTAGACTCGGACCCTCGA -
6 5'-Dabcyl), a high sensitivity duplex that assesses non-specific internal cleavage of the
7 RNA strand.
8
9

10
11
12
13
14
15 ***HIV-1 cytoprotection assay.***³⁵ The HIV Cytoprotection assay used CEM-SS cells and the
16 IIB strain of HIV-1. Briefly virus and cells were mixed in the presence of test compound
17 and incubated for 6 days. The virus was pre-titered such that control wells exhibit 70 to
18 95% loss of cell viability due to virus replication. Therefore, antiviral effect or
19 cytoprotection was observed when compounds prevent virus replication. Each assay plate
20 contained cell control wells (cells only), virus control wells (cells plus virus), compound
21 toxicity control wells (cells plus compound only), compound colorimetric control wells
22 (compound only) as well as experimental wells (compound plus cells plus virus).
23
24
25
26
27
28
29
30
31
32
33
34
35
36
37
38
39
40
41
42
43
44
45
46
47
48
49
50
51
52
53
54
55
56
57
58
59
60
Cytoprotection and compound cytotoxicity were assessed by MTS (CellTiter® 96 Reagent,
Promega, Madison WI) and the EC₅₀ (concentration inhibiting virus replication by 50%),
CC₅₀ (concentration resulting in 50% cell death) and a calculated TI (therapeutic index
CC₅₀/EC₅₀) were provided. Each assay included AZT as a positive control.

Antiviral MAGI assays. MAGI assays were carried out using P4R5 indicator cells
essentially as previously described.³⁶ P4R5 cells were cultured in 96-well microplates with
4x10³ cells per well and maintained in DMEM/10% FBS supplemented with puromycin (1
µg/ml). Cells were incubated with either 1% DMSO or varying concentrations of the drugs
for 24h and then exposed to HIV (MOI of 1.25) followed by an additional incubation period
of 48h. The extent of infection was assessed using a fluorescence-based β-galactosidase

1
2
3 detection assay, as previously described with minor modifications.⁵⁶ After the 48h
4 incubation period, cells were lysed and substrate 4-methylumbelliferyl-galactoside (MUG)
5 was added. The β -galactosidase produced during infection acts on the substrate MUG and
6 yields a fluorescent product 4-methylumbelliferone (4-MU) that could be detected
7 fluorimetrically with excitation wavelength 365 nm and emission wavelength 446 nm.

8
9
10
11
12
13
14
15 **Modeling and docking.** Molecular modeling was performed using the Schrodinger small
16 molecule drug discovery suite 2014-3. The crystal structure of PFV intasome in complex
17 with magnesium and **3** was used as a starting point (PDB code: 3S3M).⁵⁰ This model was
18 subjected to Protein Preparation Wizard⁵⁷⁻⁵⁸ (Schrödinger Inc.) in which missing hydrogens
19 atoms were added, zero-order bonds to metals were created followed by the generation of
20 metal binding states. The structure of protein was minimized using OPLS 2005 force field⁵⁹
21 to optimize hydrogen bonding network and converge heavy atoms to an rmsd of 0.3 Å. The
22 receptor grid generation tool in Maestro (Schrodinger Inc.) was used to define an active
23 site around the native ligand (**3**) to cover all the residues within 12 Å from it with both the
24 metal cofactors (Mg^{2+}) as a constraint to identify the chelating triad during docking.

25
26
27
28
29
30
31
32
33
34
35
36
37
38
39
40
41
42
43
44
45
46
47
48
49
50
51
52
53
54
55
56
57
58
59
60
All the compounds synthesized were drawn using Maestro and subjected to Lig Prep⁵⁸ to
generate conformers, possible protonation at pH of 7 ± 3 , and metal binding states that
serve as an input for docking process. All the dockings were performed using Glide XP⁶⁰
(Glide, version 6.4) mode with both the Mg^{2+} metal cofactors as a constraint. The van der
Waals radii of nonpolar atoms for each of the ligands were scaled by a factor of 0.8.

To understand the effect of observed mutations on resistance profile for **1**, **3** and the
representative compound **45**, a crystal structure of PFV intasome in complex with
magnesium and **3** was used as a starting point (PDB code: 3S3M). The observed mutants

1
2
3 were changed in the crystal structure manually using Maestro (PFV intasome numbering
4 of G209S, Y212C, Q217H and N224H corresponds to HIV intasome numbering of G140S,
5 Y143C, Q148H and N155H) followed by a protein preparation.
6
7
8
9

10 Three compounds (**1**, **3** and **45**) were drawn using Maestro and subjected to Lig Prep to
11 generate conformers, possible protonation at pH of 7 ± 3 , and metal binding states that
12 serve as an input for docking process. These compounds were docked using a similar
13 protocol as above.
14
15
16
17
18
19

20 ASSOCIATED CONTENT

21
22
23 **Supporting Information Available.** Synthesis and characterization data, including ^1H
24 NMR, ^{13}C NMR and HRMS data, of intermediates **7–23**. This material is available free of
25 charge via the Internet at <http://pubs.acs.org>.
26
27
28
29
30

31 AUTHOR INFORMATION

32 Corresponding Author

33
34
35
36 Email: wangx472@umn.edu; Phone: +1 (612) 626-7025.
37
38
39

40 ACKNOWLEDGMENTS

41
42
43 This research was supported by the National Institutes of Health (AI100890) and partially
44 by the Center for Drug Design, University of Minnesota.
45
46
47
48

49 ABBREVIATIONS USED

50
51 HIV, human immunodeficiency virus; INST, integrase strand transfer; HPD, 3-
52 hydroxypyrimidine-2,4-dione; INST, integrase strand transfer; INSTIs, integrase strand
53 transfer inhibitors; RT, reverse transcriptase; HAART, highly active antiretroviral therapy;
54
55
56
57
58
59
60

1
2
3 NRTIs, nucleoside reverse transcriptase inhibitors; NNRTIs, nonnucleoside reverse
4 transcriptase inhibitors; PIs, protease inhibitors; DKA, diketoacid; CPE, cytopathic effect;
5
6 SAR, structure-activity-relationship; MOA, mechanism of action; N-terminal domain,
7
8 NTD; catalytic core domain, CCD; C-terminal domain, CTD; PFV, prototype foamy virus.
9
10
11
12
13
14
15
16
17
18
19
20
21
22
23
24
25
26
27
28
29
30
31
32
33
34
35
36
37
38
39
40
41
42
43
44
45
46
47
48
49
50
51
52
53
54
55
56
57
58
59
60

References

1. Kinch, M. S.; Patridge, E., An analysis of FDA-approved drugs for infectious disease: HIV/AIDS drugs. *Drug Discov. Today* **2014**, *19*, 1510-1513.
2. Barouch, D. H.; Deeks, S. G., Immunologic strategies for HIV-1 remission and eradication. *Science* **2014**, *345*, 169-174.
3. Chun, T. W.; Fauci, A. S., HIV reservoirs: pathogenesis and obstacles to viral eradication and cure. *AIDS* **2012**, *26*, 1261-1268.
4. Bagasra, O., A unified concept of HIV latency. *Expert Opin. Biol. Ther.* **2006**, *6*, 1135-1149.
5. Chun, T.-W.; Stuyver, L.; Mizell, S. B.; Ehler, L. A.; Mican, J. A. M.; Baseler, M.; Lloyd, A. L.; Nowak, M. A.; Fauci, A. S., Presence of an inducible HIV-1 latent reservoir during highly active antiretroviral therapy. *Proc. Natl. Acad. Sci. USA* **1997**, *94*, 13193-13197.
6. Finzi, D.; Hermankova, M.; Pierson, T.; Carruth, L. M.; Buck, C.; Chaisson, R. E.; Quinn, T. C.; Chadwick, K.; Margolick, J.; Brookmeyer, R.; Gallant, J.; Markowitz, M.; Ho, D. D.; Richman, D. D.; Siliciano, R. F., Identification of a reservoir for HIV-1 in patients on highly active antiretroviral therapy. *Science* **1997**, *278*, 1295-1300.
7. Pommier, Y.; Johnson, A. A.; Marchand, C., Integrase inhibitors to treat HIV/AIDS. *Nat. Rev. Drug Discovery* **2005**, *4*, 236-248.
8. Cotelle, P., Patented HIV-1 integrase inhibitors (1998-2005). *Recent Pat. Anti-Infect. Drug Discovery* **2006**, *1*, 1-15.

- 1
2
3
4
5
6
7
8
9
10
11
12
13
14
15
16
17
18
19
20
21
22
23
24
25
26
27
28
29
30
31
32
33
34
35
36
37
38
39
40
41
42
43
44
45
46
47
48
49
50
51
52
53
54
55
56
57
58
59
60
9. Henao-Mejia, J.; Goez, Y.; Patino, P.; Rugeles, M. T., Diketo acids derivatives as integrase inhibitors: the war against the acquired immunodeficiency syndrome. *Recent Pat. Anti-Infect. Drug Discovery* **2006**, *1*, 255-265.
 10. Dubey, S.; Satyanarayana, Y. D.; Lavania, H., Development of integrase inhibitors for treatment of AIDS: An overview. *Eur. J. Med. Chem.* **2007**, *42*, 1159-1168.
 11. Marchand, C.; Maddali, K.; Metifiot, M.; Pommier, Y., HIV-1 IN inhibitors: 2010 update and perspectives. *Curr. Top. Med. Chem.* **2009**, *9*, 1016-1037.
 12. Dayam, R.; Sanchez, T.; Neamati, N., Diketo acid pharmacophore. 2. discovery of structurally diverse inhibitors of HIV-1 integrase. *J. Med. Chem.* **2005**, *48*, 8009-8015.
 13. Dayam, R.; Sanchez, T.; Clement, O.; Shoemaker, R.; Sei, S.; Neamati, N., b-Diketo acid pharmacophore hypothesis. 1. discovery of a novel class of HIV-1 integrase inhibitors. *J. Med. Chem.* **2005**, *48*, 111-120.
 14. Deng, J.; Sanchez, T.; Neamati, N.; Briggs, J. M., Dynamic pharmacophore model optimization: identification of novel HIV-1 integrase inhibitors. *J. Med. Chem.* **2006**, *49*, 1684-1692.
 15. Barreca, M. L.; Ferro, S.; Rao, A.; De Luca, L.; Zappala, M.; Monforte, A.-M.; Debyser, Z.; Witvrouw, M.; Chimirri, A., Pharmacophore-based design of HIV-1 integrase strand-transfer inhibitors. *J. Med. Chem.* **2005**, *48*, 7084-7088.
 16. Mustata, G. I.; Brigo, A.; Briggs, J. M., HIV-1 integrase pharmacophore model derived from diverse classes of inhibitors. *Bioorg. Med. Chem. Lett.* **2004**, *14*, 1447-1454.
 17. Carlson, H. A.; Masukawa, K. M.; Rubins, K.; Bushman, F. D.; Jorgensen, W. L.; Lins, R. D.; Briggs, J. M.; McCammon, J. A., Developing a dynamic pharmacophore model for HIV-1 integrase. *J. Med. Chem.* **2000**, *43*, 2100-2114.

- 1
2
3
4
5
6
7
8
9
10
11
12
13
14
15
16
17
18
19
20
21
22
23
24
25
26
27
28
29
30
31
32
33
34
35
36
37
38
39
40
41
42
43
44
45
46
47
48
49
50
51
52
53
54
55
56
57
58
59
60
18. Cocohoba, J.; Dong, B. J., Raltegravir: the first HIV integrase inhibitor. *Clin. Ther.* **2008**, *30*, 1747-1765.
 19. Summa, V.; Petrocchi, A.; Bonelli, F.; Crescenzi, B.; Donghi, M.; Ferrara, M.; Fiore, F.; Gardelli, C.; Gonzalez Paz, O.; Hazuda, D. J.; Jones, P.; Kinzel, O.; Laufer, R.; Monteagudo, E.; Muraglia, E.; Nizi, E.; Orvieto, F.; Pace, P.; Pescatore, G.; Scarpelli, R.; Stillmock, K.; Witmer, M. V.; Rowley, M., Discovery of raltegravir, a potent, selective orally bioavailable HIV-Integrase inhibitor for the treatment of HIV-AIDS infection. *J. Med. Chem.* **2008**, *51*, 5843-5855.
 20. Shimura, K.; Kodama, E. N., Elvitegravir: a new HIV integrase inhibitor. *Antiviral Chem. Chemother.* **2009**, *20*, 79-85.
 21. Vandekerckhove, L., GSK-1349572, a novel integrase inhibitor for the treatment of HIV infection. *Curr. Opin. Invest. Drugs* **2010**, *11*, 203-212.
 22. Min, S.; Song, I.; Borland, J.; Chen, S.; Lou, Y.; Fujiwara, T.; Piscitelli, S. C., Pharmacokinetics and safety of S/GSK1349572, a next-generation HIV integrase inhibitor, in healthy volunteers. *Antimicrob. Agents Chemother.* **2009**, *54*, 254-258.
 23. Shafer, R. W., Rationale and uses of a public HIV drug-resistance database. *J. Infect. Dis.* **2006**, *194 Suppl 1*, S51-8.
 24. Tang, J.; Maddali, K.; Dreis, C. D.; Sham, Y. Y.; Vince, R.; Pommier, Y.; Wang, Z., N-3 hydroxylation of pyrimidine-2,4-diones yields dual inhibitors of HIV reverse transcriptase and integrase. *ACS Med. Chem. Lett.* **2011**, *2*, 63-67.
 25. Tang, J.; Maddali, K.; Dreis, C. D.; Sham, Y. Y.; Vince, R.; Pommier, Y.; Wang, Z. Q., 6-Benzoyl-3-hydroxypyrimidine-2,4-diones as dual inhibitors of HIV reverse transcriptase and integrase. *Bioorg. Med. Chem. Lett.* **2011**, *21*, 2400-2402.

- 1
2
3
4
5
6
7
8
9
10
11
12
13
14
15
16
17
18
19
20
21
22
23
24
25
26
27
28
29
30
31
32
33
34
35
36
37
38
39
40
41
42
43
44
45
46
47
48
49
50
51
52
53
54
55
56
57
58
59
60
26. Tang, J.; Maddali, K.; Metifiot, M.; Sham, Y. Y.; Vince, R.; Pommier, Y.; Wang, Z. Q., 3-Hydroxypyrimidine-2,4-diones as an inhibitor scaffold of HIV integrase. *J. Med. Chem.* **2011**, *54*, 2282-2292.
27. Tang, J.; Maddali, K.; Dreis, C. D.; Sham, Y. Y.; Vince, R.; Pommier, Y.; Wang, Z. Q., 6-Benzoyl-3-hydroxypyrimidine-2,4-diones as dual inhibitors of HIV reverse transcriptase and integrase. *Bioorg. Med. Chem. Lett.* **2011**, *21*, 2400-2402.
28. Vernekar, S. K.; Liu, Z.; Nagy, E.; Miller, L.; Kirby, K. A.; Wilson, D. J.; Kankanala, J.; Sarafianos, S. G.; Parniak, M. A.; Wang, Z., Design, synthesis, biochemical, and antiviral evaluations of C6 benzyl and C6 biarylmethyl substituted 2-hydroxyisoquinoline-1,3-diones: dual inhibition against HIV reverse transcriptase-associated RNase H and polymerase with antiviral activities. *J. Med. Chem.* **2015**, *58*, 651-664.
29. Mai, X.; Lu, X. S.; Xia, H. Y.; Cao, Y. S.; Liao, Y. J.; Lv, X. L., Synthesis, antitumor evaluation and crystal structure of hydroxyurea derivatives. *Chem. Pharm. Bull.* **2010**, *58*, 94-97.
30. Stadlbauer, W.; Badawey, E. S.; Hojas, G.; Roschger, P.; Kappe, T., Malonates in cyclocondensation reactions. *Molecules* **2001**, *6*, 338-352.
31. Arnott, E. A.; Chan, L. C.; Cox, B. G.; Meyrick, B.; Phillips, A., POCl₃ chlorination of 4-quinazolones. *J. Org. Chem.* **2011**, *76*, 1653-1661.
32. Kotera, M.; Ishii, K.; Tamura, O.; Sakamoto, M., 1,3-dipolar cycloadditions of photoinduced carbonyl ylides. Part 2. Photoreactions of alpha,beta-unsaturated gamma,delta-epoxy dinitriles and ethyl vinyl ether. *J. Chem. Soc. Perkin Trans. 1* **1998**, 313-318.
33. Lee, I. Y.; Lee, J. Y.; Gong, Y. D., Microwave-assisted facile one-step carbamoylation of 6-aminouracils. *Synthesis* **2005**, 2713-2717.

- 1
2
3
4
5
6
7
8
9
10
11
12
13
14
15
16
17
18
19
20
21
22
23
24
25
26
27
28
29
30
31
32
33
34
35
36
37
38
39
40
41
42
43
44
45
46
47
48
49
50
51
52
53
54
55
56
57
58
59
60
34. Fletcher, S.; Gunning, P. T., Mild, efficient and rapid O-debenzylation of ortho-substituted phenols with trifluoroacetic acid. *Tetrahedron Lett.* **2008**, *49*, 4817-4819.
35. Mosmann, T., Rapid colorimetric assay for cellular growth and survival: application to proliferation and cytotoxicity assays. *J. Immunol. Methods* **1983**, *65*, 55-63.
36. Sirivolu, V. R.; Vernekar, S. K. V.; Ilina, T.; Myshakina, N. S.; Parniak, M. A.; Wang, Z. Q., Clicking 3'-azidothymidine into novel potent inhibitors of human immunodeficiency virus. *J. Med. Chem.* **2013**, *56*, 8765-8780.
37. Kimpton, J.; Emerman, M., Detection of replication-competent and pseudotyped human immunodeficiency virus with a sensitive cell line on the basis of activation of an integrated beta-galactosidase gene. *J. Virol.* **1992**, *66*, 2232-2239.
38. Metifiot, M.; Marchand, C.; Maddali, K.; Pommier, Y., Resistance to integrase inhibitors. *Viruses* **2010**, *2*, 1347-1366.
39. Metifiot, M.; Maddali, K.; Naumova, A.; Zhang, X.; Marchand, C.; Pommier, Y., Biochemical and pharmacological analyses of HIV-1 integrase flexible loop mutants resistant to raltegravir. *Biochemistry* **2010**, *49*, 3715-3722.
40. da Silva, D.; Van Wesenbeeck, L.; Breilh, D.; Reigadas, S.; Anies, G.; Van Baelen, K.; Morlat, P.; Neau, D.; Dupon, M.; Wittkop, L.; Fleury, H.; Masquelier, B., HIV-1 resistance patterns to integrase inhibitors in antiretroviral-experienced patients with virological failure on raltegravir-containing regimens. *J. Antimicrob. Chemother.* **2010**, *65*, 1262-1269.
41. Reuman, E. C.; Bachmann, M. H.; Varghese, V.; Fessel, W. J.; Shafer, R. W., Panel of prototypical raltegravir-resistant infectious molecular clones in a novel integrase-deleted cloning vector. *Antimicrob. Agents Chemother.* **2010**, *54*, 934-936.

- 1
2
3
4 42. Fantauzzi, A.; Mezzaroma, I., Dolutegravir: clinical efficacy and role in HIV therapy. *Ther.*
5
6 *Adv. Chronic Dis.* **2014**, *5*, 164-177.
7
8 43. Nowotny, M., Retroviral integrase superfamily: the structural perspective. *EMBO Rep.*
9
10 **2009**, *10*, 144-151.
11
12 44. Esposito, D.; Craigie, R., HIV integrase structure and function. *Adv. Virus Res.* **1999**, *52*,
13
14 319-333.
15
16 45. Goldgur, Y.; Dyda, F.; Hickman, A. B.; Jenkins, T. M.; Craigie, R.; Davies, D. R., Three
17
18 new structures of the core domain of HIV-1 integrase: an active site that binds magnesium.
19
20
21 *Proc. Natl. Acad. Sci. USA.* **1998**, *95*, 9150-9154.
22
23 46. Dyda, F.; Hickman, A. B.; Jenkins, T. M.; Engelman, A.; Craigie, R.; Davies, D. R., Crystal
24
25 structure of the catalytic domain of HIV-1 integrase: similarity to other polynucleotidyl
26
27 transferases. *Science* **1994**, *266*, 1981-1986.
28
29 47. O'Brien, C., HIV integrase structure catalyzes drug search. *Science* **1994**, *266*, 1946.
30
31 48. Hare, S.; Gupta, S. S.; Valkov, E.; Engelman, A.; Cherepanov, P., Retroviral intasome
32
33 assembly and inhibition of DNA strand transfer. *Nature* **2010**, *464*, 232-236.
34
35 49. Hare, S.; Vosb, A. M.; Claytonb, R. F.; Thuringb, J. W.; Cummingsb, M. D.; Cherepanov,
36
37 P., Molecular mechanisms of retroviral integrase inhibition and the evolution of viral
38
39 resistance. *Proc. Natl. Acad. Sci. USA* **2010**, *157*, 20057-20062.
40
41 50. Hare, S., Smith, S.J., Metifiot, M., Jaxa-Chamiec, A., Pommier, Y., Hughes,
42
43 S.H., Cherepanov, P. Structural and functional analyses of the second-generation integrase
44
45 strand transfer inhibitor dolutegravir (S/GSK1349572). *Mol. Pharmacol.* **2011**, *80*, 565-
46
47 572.
48
49
50
51
52
53
54
55
56
57
58
59
60

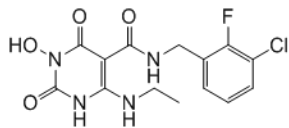
- 1
2
3
4
5
6
7
8
9
10
11
12
13
14
15
16
17
18
19
20
21
22
23
24
25
26
27
28
29
30
31
32
33
34
35
36
37
38
39
40
41
42
43
44
45
46
47
48
49
50
51
52
53
54
55
56
57
58
59
60
51. Krishnan, L.; Li, X.; Naraharisetty, H. L.; Hare, S.; Cherepanov, P.; Engelman, A., Structure-based modeling of the functional HIV-1 intasome and its inhibition. *Proc. Natl. Acad. Sci. U. S. A.* **2010**, *107*, 15910-15915.
52. Wang, Z.; Bennett, E. M.; Wilson, D. J.; Salomon, C.; Vince, R., Rationally designed dual inhibitors of HIV reverse transcriptase and integrase. *J. Med. Chem.* **2007**, *50*, 3416-3419.
53. Leh, H.; Brodin, P.; Bischerour, J.; Deprez, E.; Tauc, P.; Brochon, J. C.; LeCam, E.; Coulaud, D.; Auclair, C.; Mouscadet, J. F., Determinants of Mg²⁺-dependent activities of recombinant human immunodeficiency virus type 1 integrase. *Biochemistry* **2000**, *39*, 9285-9294.
54. Semenova, E. A.; Johnson, A. A.; Marchand, C.; Davis, D. A.; Yarchoan, R.; Pommier, Y., Preferential inhibition of the magnesium-dependent strand transfer reaction of HIV-1 integrase by α -hydroxytropolones. *Mol. Pharmacol.* **2006**, *69*, 1454-1460.
55. Parniak, M. A.; Min, K. L.; Budihas, S. R.; Le Grice, S. F.; Beutler, J. A., A fluorescence-based high-throughput screening assay for inhibitors of human immunodeficiency virus-1 reverse transcriptase-associated ribonuclease H activity. *Anal. Biochem.* **2003**, *322*, 33-39.
56. Abram, M. E.; Parniak, M. A., Virion instability of human immunodeficiency virus type 1 reverse transcriptase (RT) mutated in the protease cleavage site between RT p51 and the RT RNase H domain. *J. Virol.* **2005**, *79*, 11952-11961.
57. Sastry, G. M.; Adzhigirey, M.; Day, T.; Annabhimoju, R.; Sherman, W. Protein and ligand preparation: parameters, protocols, and influence on virtual screening enrichments. *J. Comput. Aided Mol. Des.* **2013**, *27*, 221-234.
58. Schrödinger Release 2014-3: Schrödinger Suite 2014-3 Protein Preparation Wizard; Epik version 2.9, Schrödinger, LLC, New York, NY, **2014**; Impact version 6.4, Schrödinger,

1
2
3 LLC, New York, NY, **2014**; Prime version 3.7, Schrödinger, LLC, New York, NY, **2014**.

4
5 In.

- 6
7
8 59. Jorgensen, W. L.; Maxwell, D. S.; TiradoRives, J. Development and testing of the OPLS
9 all-atom force field on conformational energetics and properties of organic liquids. *J. Am.*
10 *Chem. Soc.* **1996**, *118*, 11225-11236
11
12
13
14
15 60. Friesner, R. A.; Banks, J. L.; Murphy, R. B.; Halgren, T. A.; Klicic, J. J.; Mainz, D. T.;
16 Repasky, M. P.; Knoll, E. H.; Shelley, M.; Perry, J. K.; Shaw, D. E.; Francis, P.; Shenkin,
17 P. S., Glide: a new approach for rapid, accurate docking and scoring. 1. Method and
18 assessment of docking accuracy. *J. Med. Chem.* **2004**, *47*, 1139-1149.
19
20
21
22
23
24
25
26
27
28
29
30
31
32
33
34
35
36
37
38
39
40
41
42
43
44
45
46
47
48
49
50
51
52
53
54
55
56
57
58
59
60

TOC Graphic



INST IC_{50} = 0.021 μ M
RNase H IC_{50} = 0.029 μ M
HIV-1 EC_{50} = 0.015 μ M
 CC_{50} = 18 μ M
MW = 357

